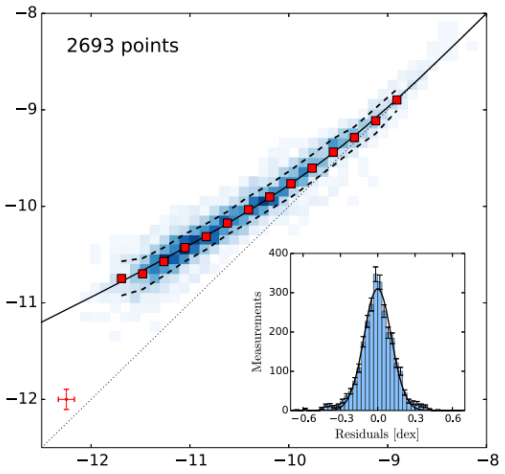

McGaugh, Lelli & Schombert 2016

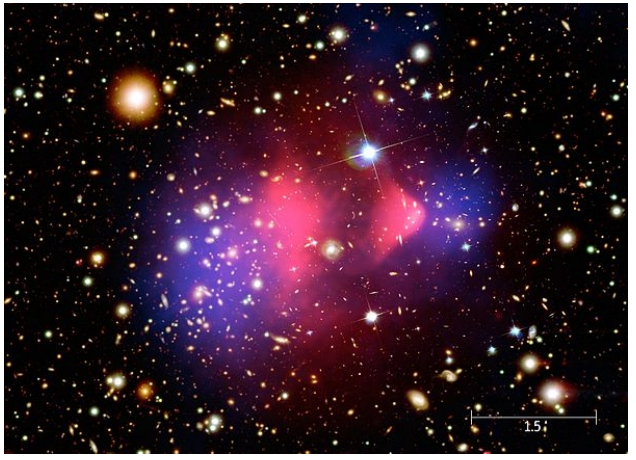

Bullet Cluster, credits: NASA/CXC/M. Weiss

Milgromian dynamics (MOND): Theoretical motivations & cosmological context

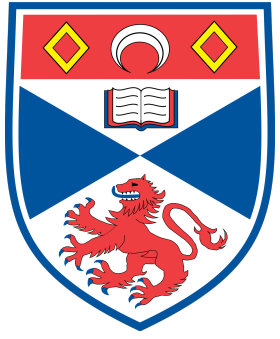

Astrophysics > Cosmology and Nongalactic Astrophysics

[Submitted on 13 Oct 2021 (v1), last revised 24 Nov 2021 (this version, v3)]

From galactic bars to the Hubble tension — weighing up the astrophysical evidence for Milgromian gravity

Indranil Banik, Hongsheng Zhao

Astronomical observations reveal a major deficiency in our understanding of physics — the detectable mass is insufficient to explain the observed motions in a huge variety of systems given our current understanding of gravity, Einstein's General theory of Relativity (GR). This missing gravity problem may indicate a breakdown of GR at low accelerations, as postulated by Milgromian dynamics (MOND). We review the MOND theory and its consequences, including in a cosmological context where we advocate a hybrid approach involving light sterile neutrinos to address MOND's cluster-scale issues. We then test the novel predictions of MOND using evidence from galaxies, galaxy groups, galaxy clusters, and the large scale structure of the Universe. We also consider whether the standard cosmological paradigm (ΛCDM) can explain the observations, and review several previously published highly significant falsifications of it. Our overall assessment considers both the extent to which the data agree with each theory and how much flexibility each has when accommodating the data, with the gold standard being a clear a priori prediction not informed by the data in question. We also consider some future tests, including on scales much smaller than galaxies. Our conclusion is that MOND is favoured by a wealth of data across a huge range of astrophysical scales, ranging from the kpc scales of galactic bars to the Gpc scale of the local supervoid and the Hubble tension, which is alleviated in MOND through enhanced cosmic variance.

Speaker: Indranil Banik, University of Saint Andrews

Galaxies

Visible mass X Newtonian Gravity = Acceleration

- **The observed acceleration is discrepant with this prediction**

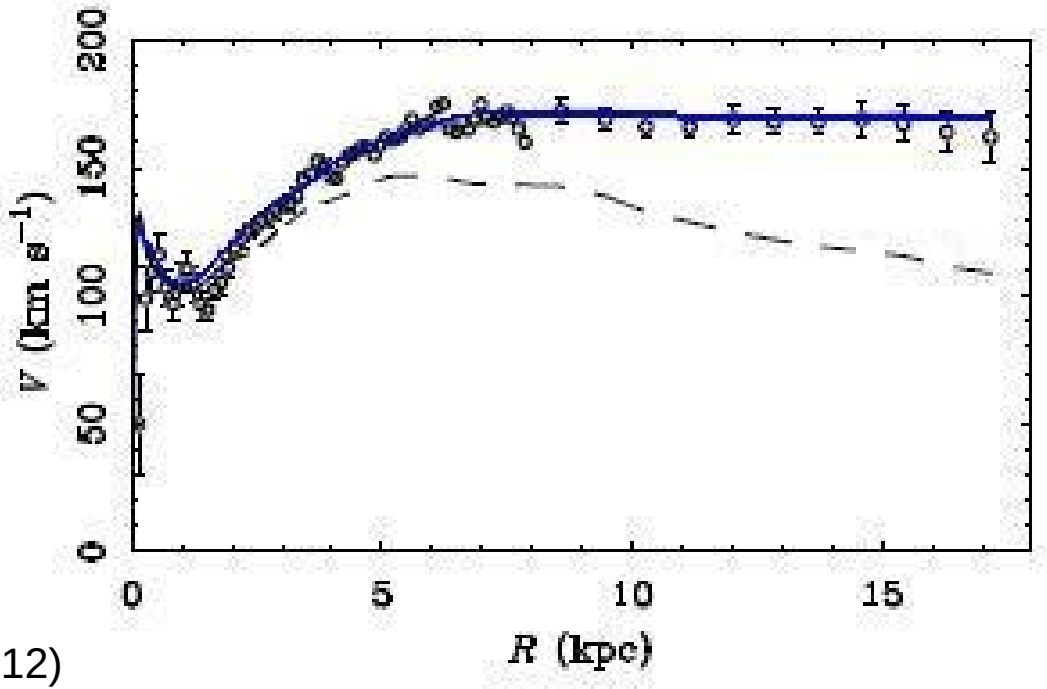

Living Reviews in Relativity, 15, 10 (2012)

Galaxies

Visible mass X Newtonian Gravity = Acceleration

- **The observed acceleration is discrepant with this prediction**

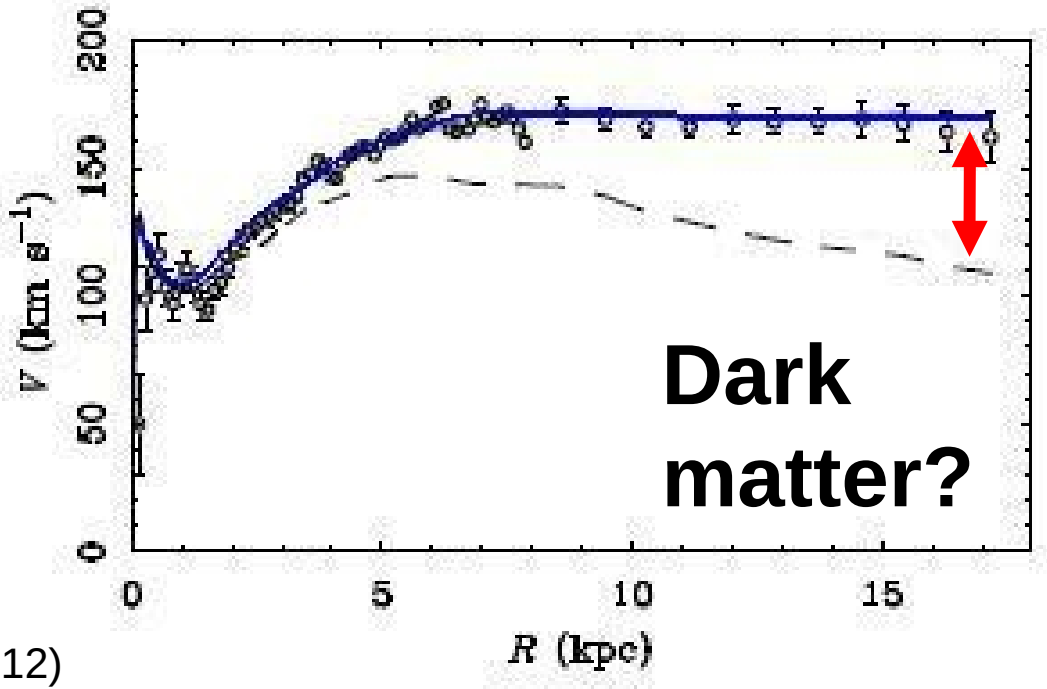

Living Reviews in Relativity, 15, 10 (2012)

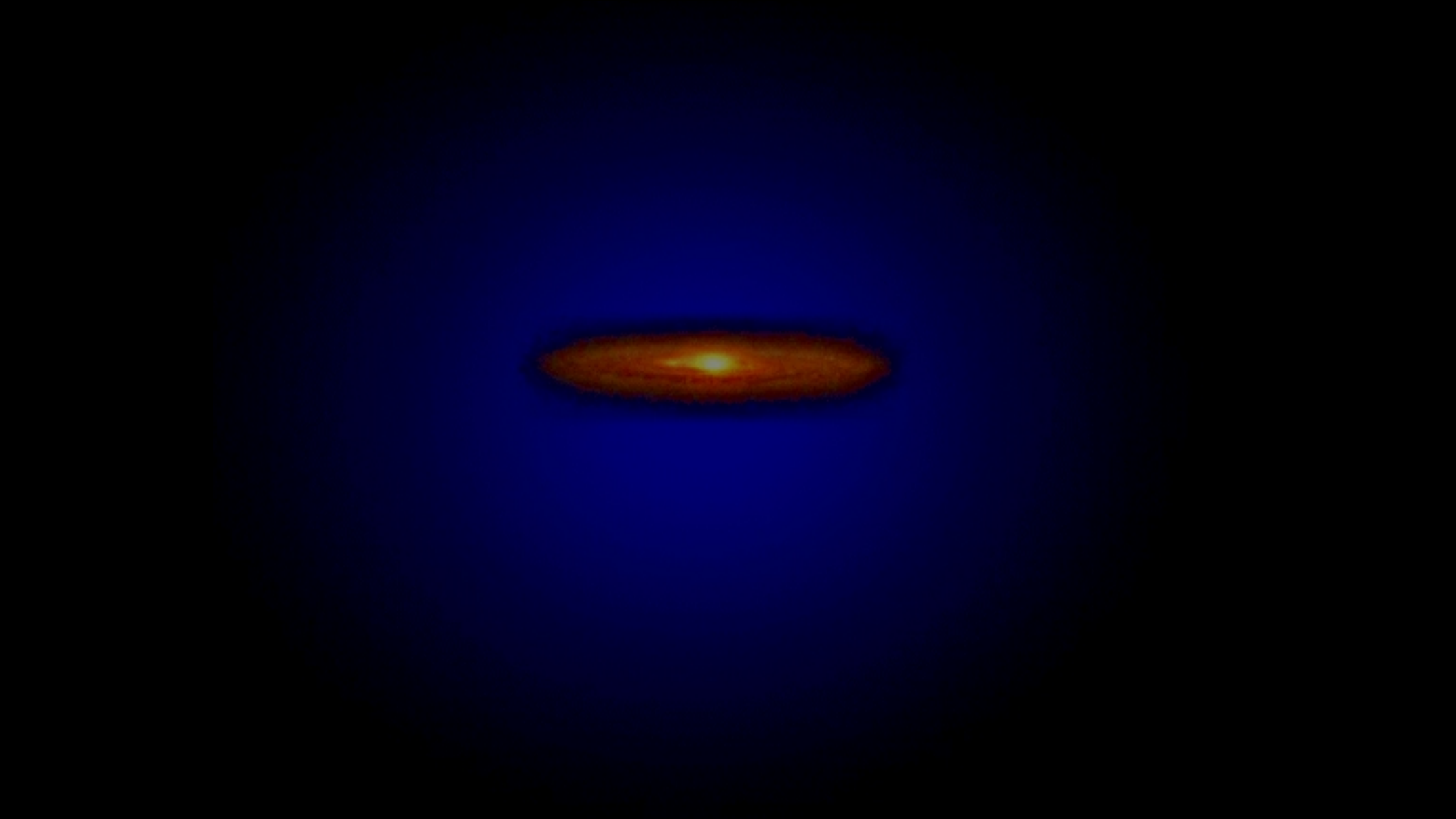

No direct evidence

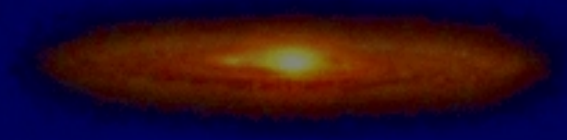

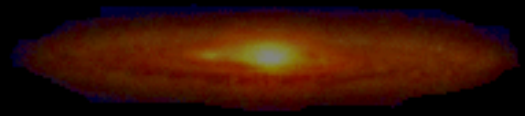

Newtonian gravity

- **The circular rotation speed around a mass is given by**

$$g = \frac{GM}{r^2} = \frac{v^2}{r}$$

- **If $v \approx c$, relativity becomes important and the theory fails (e.g., near black holes)**
- **What about quantum mechanics?**

The classical approximation

- **Arbitrarily high accuracy in position and velocity measurements impossible**
- **Classical theories assume this *is* possible**

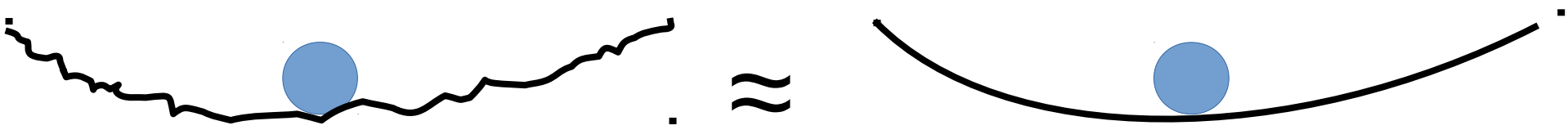

The classical approximation

- **Arbitrarily high accuracy in position and velocity measurements impossible**
- **Classical theories assume this *is* possible**

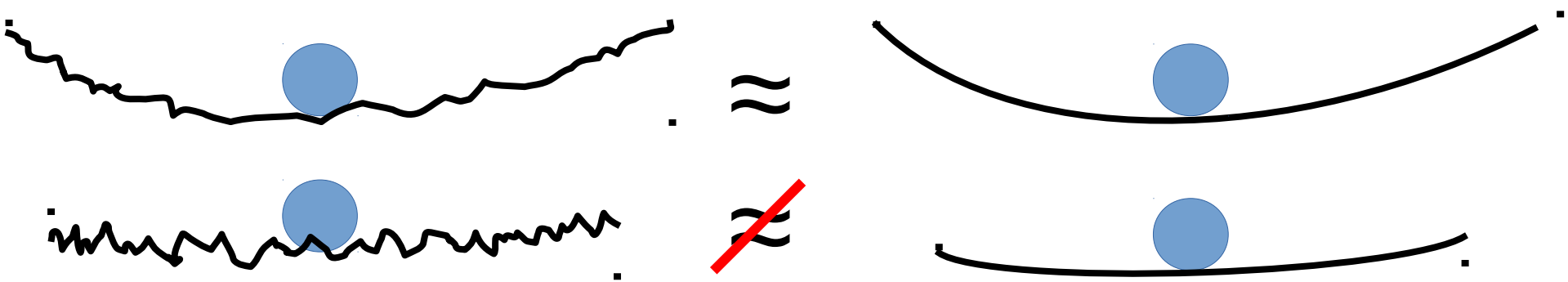

- **Curvature (i.e. acceleration) so small in second panel that ignoring fluctuations is questionable**

Quantum effects

- **Curvature uncertain and not constant**

  → gravitational waves: vacuum carries energy density

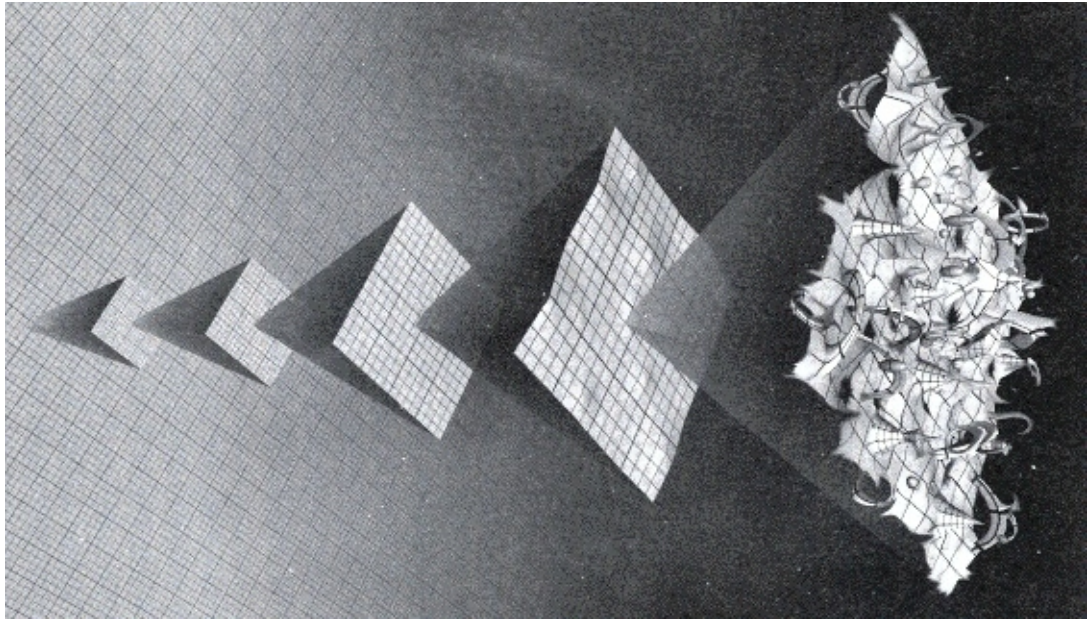

Quantum spacetime

- **Empty space has small but non-zero minimum energy**
- **On large scales, this causes the Universe to accelerate**

  → dark energy (measurable)
- **Use dark energy density to estimate when quantum effects overwhelm classical (mean) gravitational field**

  (e.g. Milgrom 1999, Pazy 2013, Verlinde 2016, Smolin 2017, Bagchi & Fring 2019, Senay+ 2021)

$$\frac{g^2}{8\pi G} = \rho_{vac} \quad \Leftrightarrow \quad g = 9\times10^{-10}\, m/s^2$$

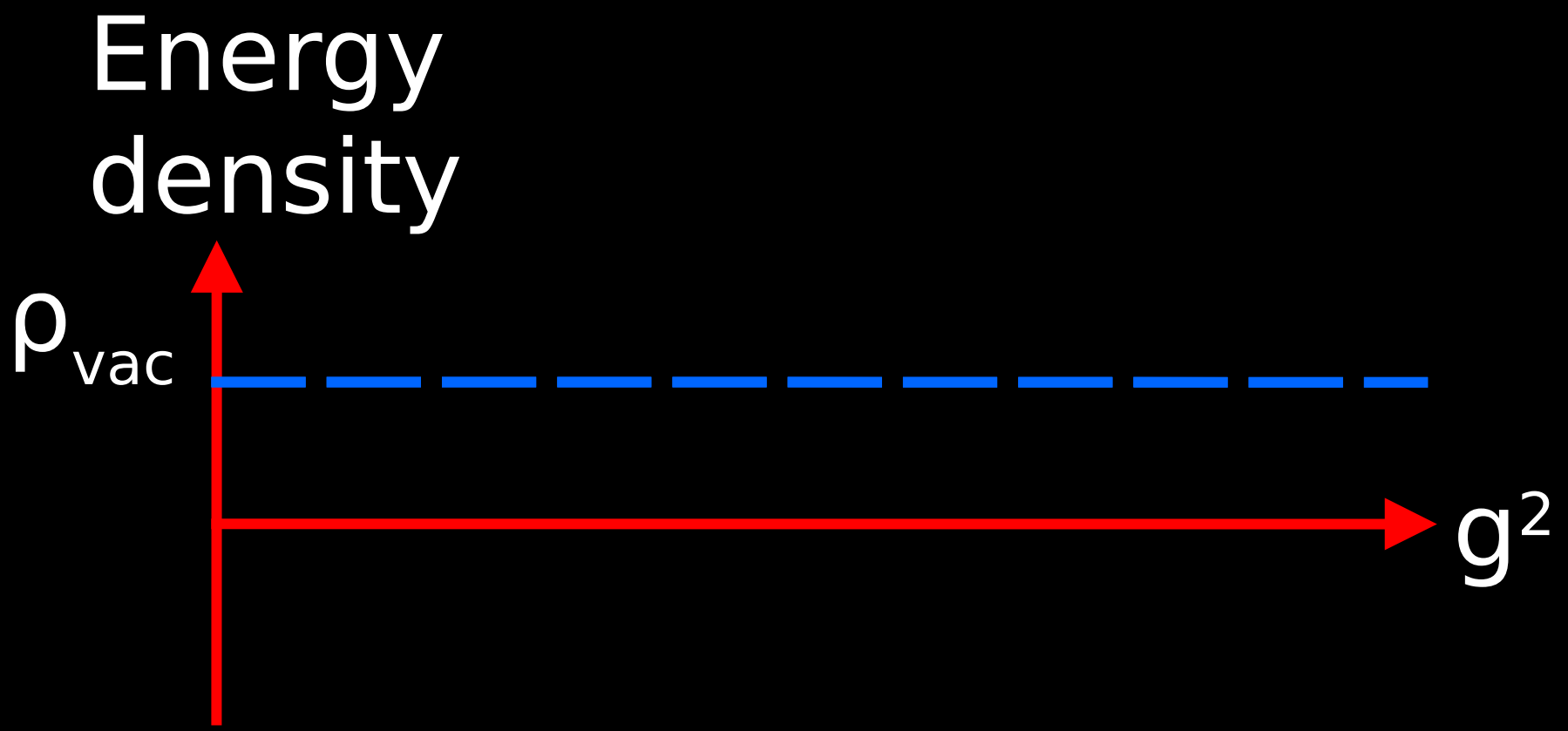
Energy
density
ρ_{vac}
g^2

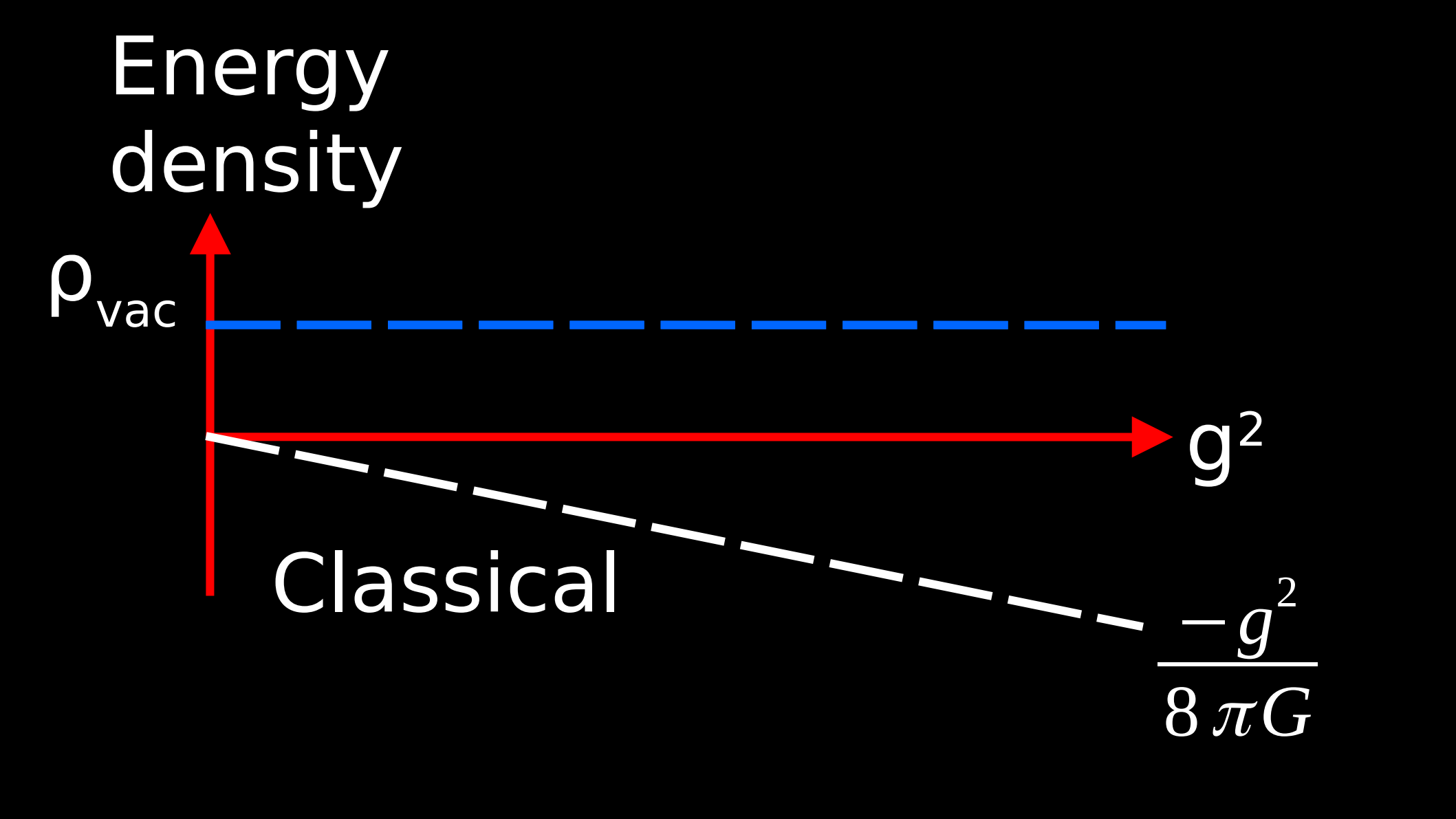
Energy
density
ρ_{vac}
g^2
Classical
$\frac{-g^2}{8\pi G}$

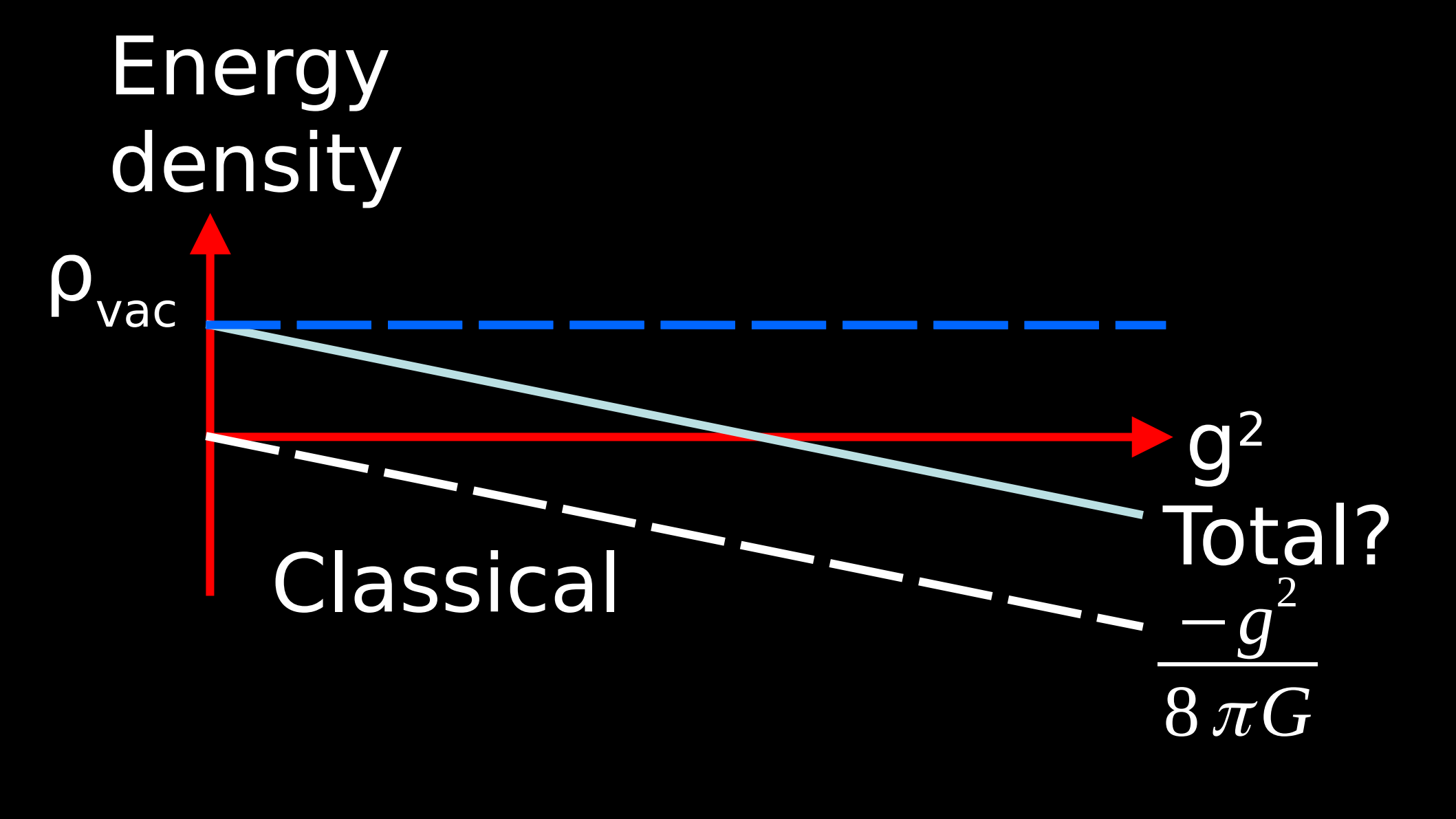
Energy
density
ρ_{vac}
g^2
Total?
Classical
$\frac{-g^2}{8\pi G}$

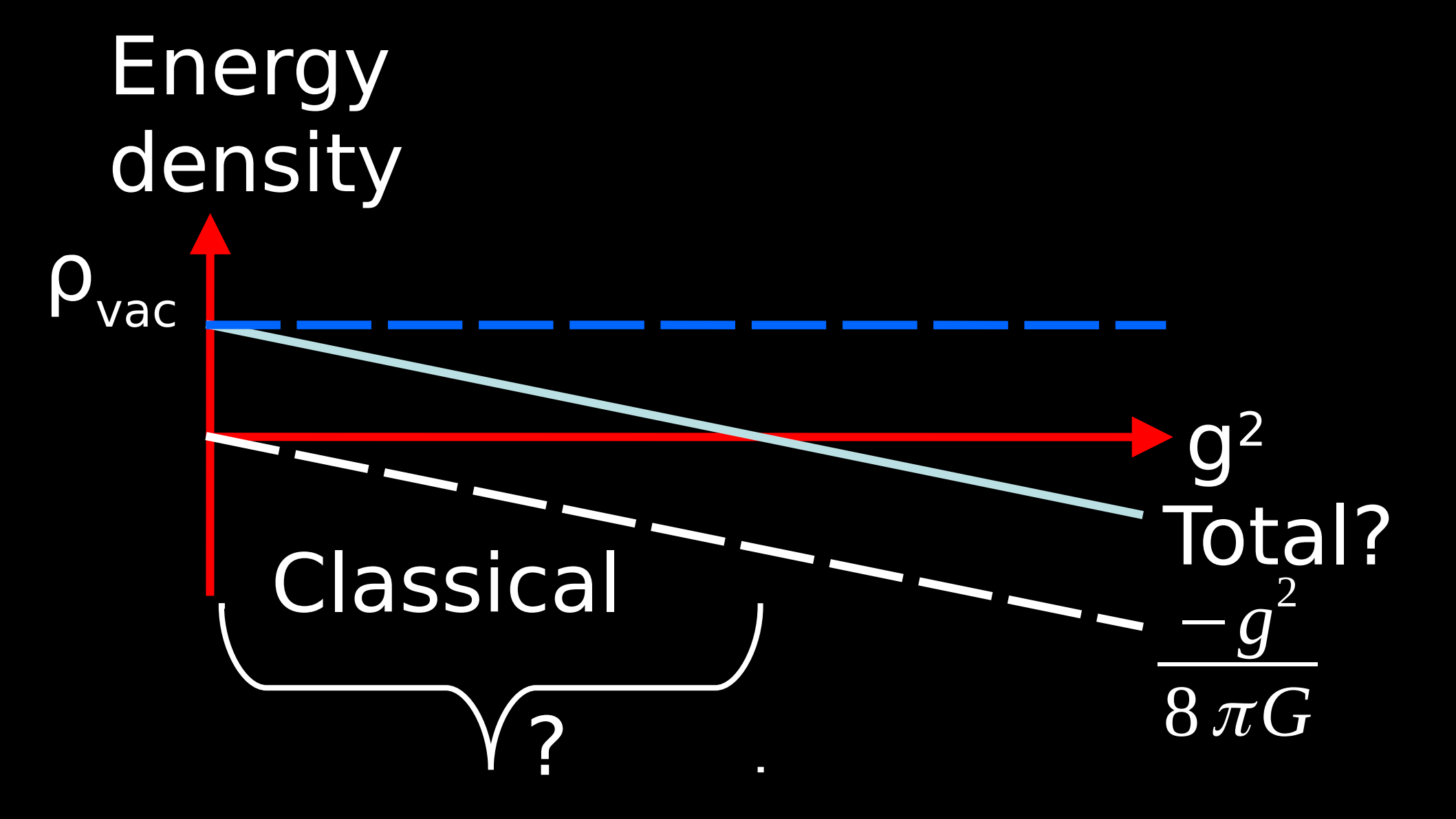
Energy
density
ρ_{vac}
g^2
Total?
$\frac{-g^2}{8\pi G}$
Classical
?

What if g < 9e-10 m/s² ?

- **Quantum gravity effects should become important (ignoring ‘roughness’ is a bad idea)**
- **Classical theories like General Relativity (leading to Newtonian dynamics) can’t really be expected to work any more**

  ⇒ Newtonian gravity likely fails, with the discrepancy larger at smaller accelerations

  ⇒ Acceleration (energy density)-dependent discrepancy with classical theory may be a signature of quantum effects

Constraints from disk galaxies

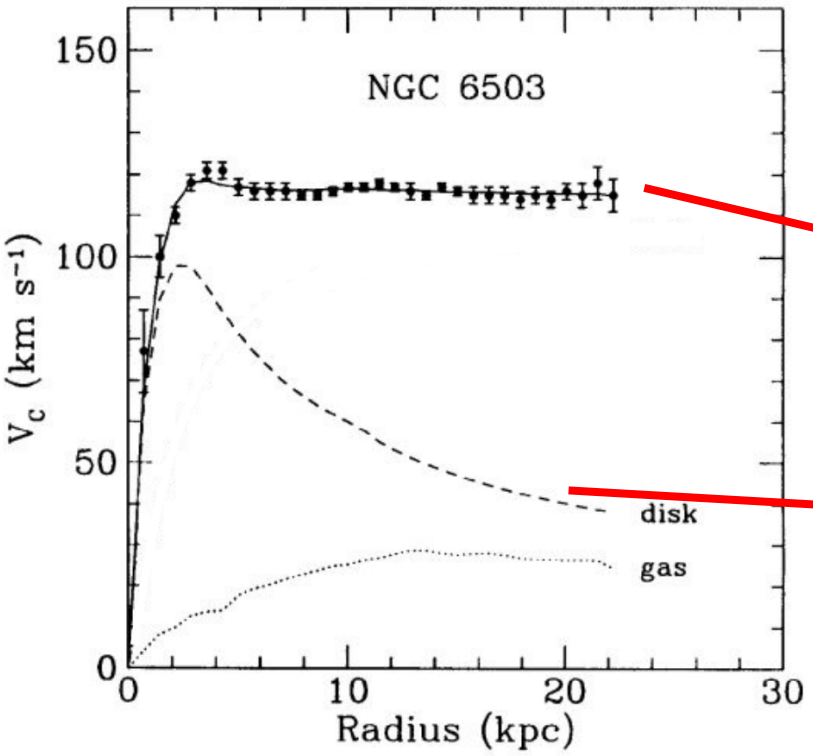

Freese 2008

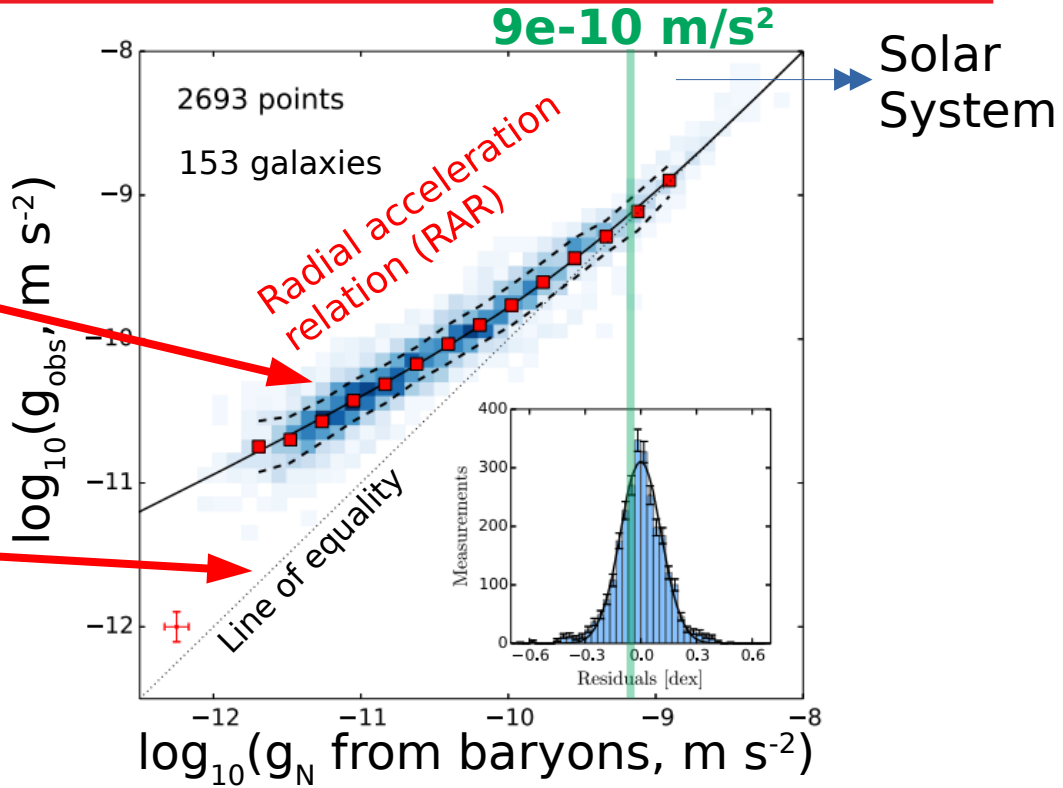

McGaugh, Lelli, Schombert 2016

Constraints from elliptical galaxies

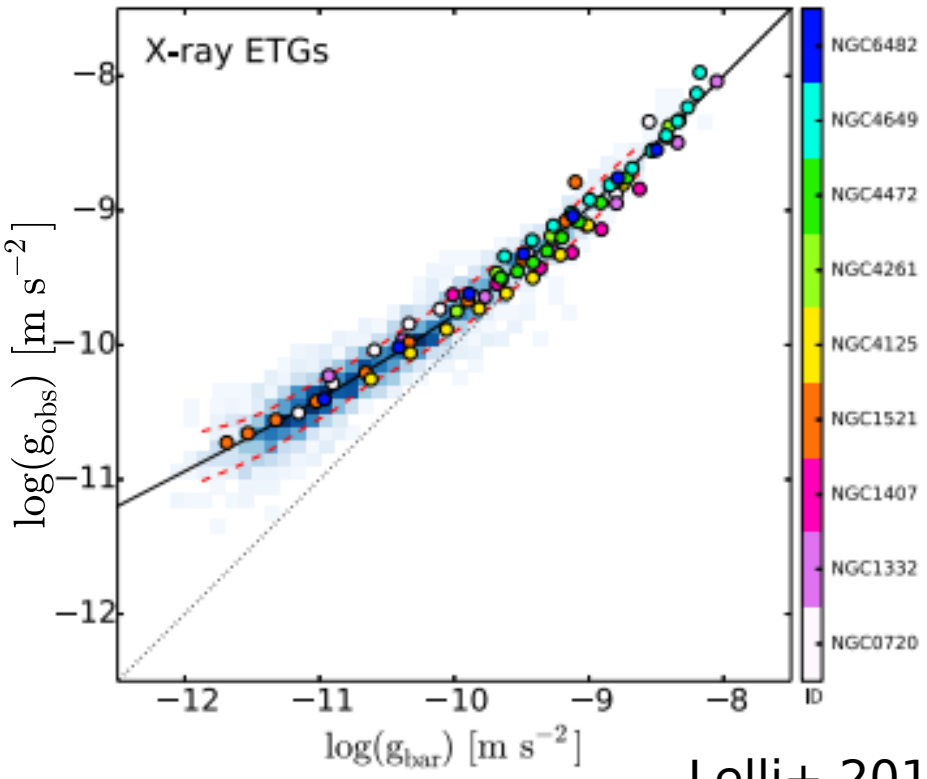

Lelli+ 2017

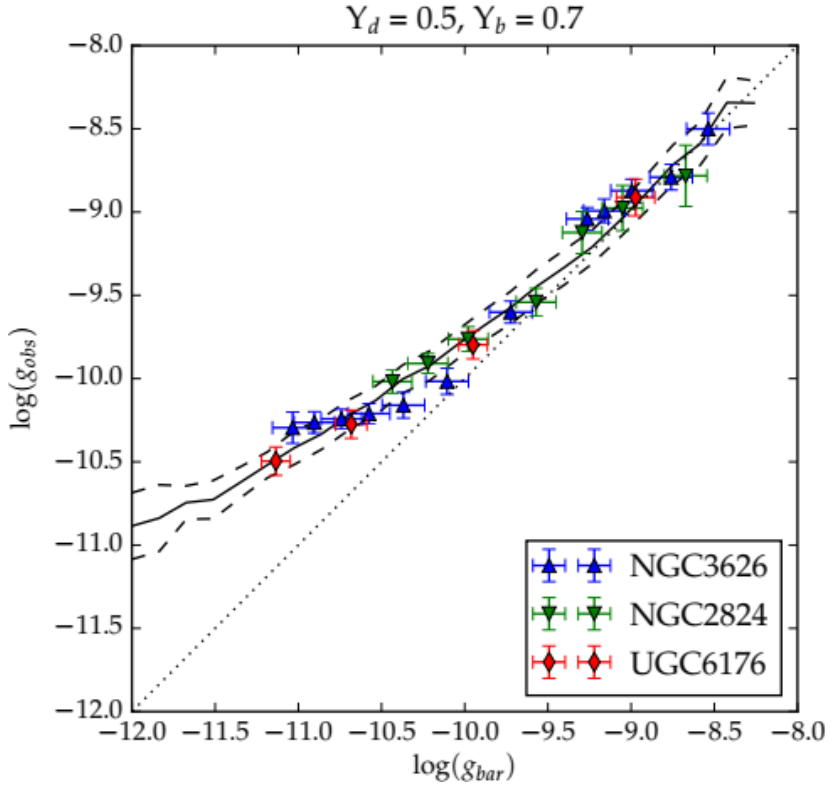

Shelest & Lelli 2020

Local Group satellite planes

MW satellite galaxies lie within a thin plane (Pawlowski & Kroupa 2013, 2020). Analogous situation for M31 (Ibata+ 2013)

Galaxies observed forming within tidal tails (Mirabel+ 1992)

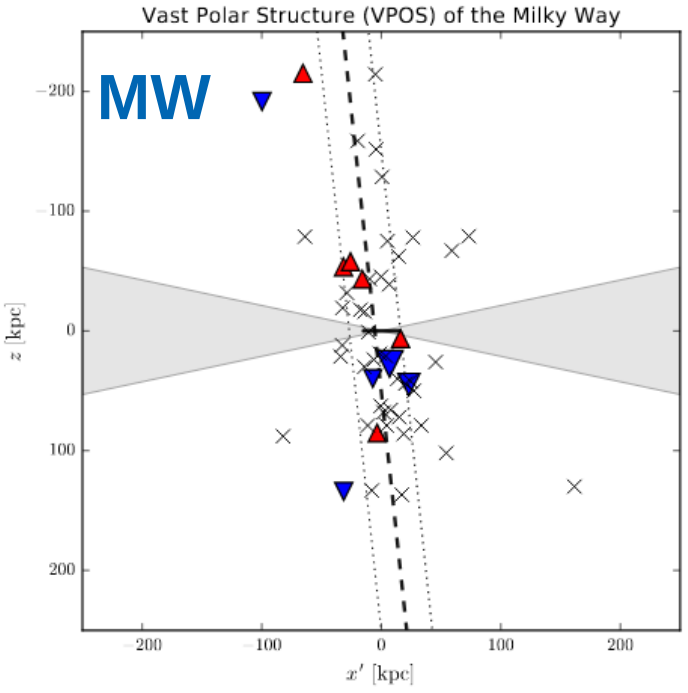

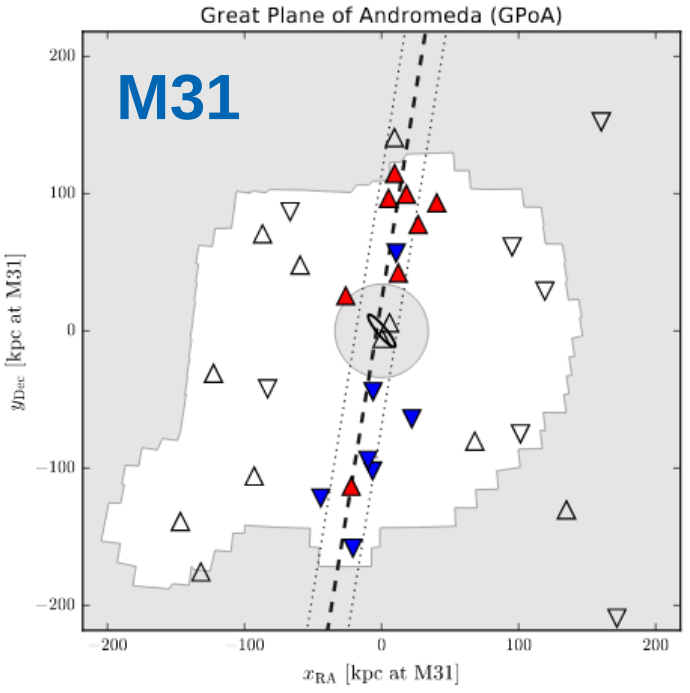

Local Group satellite planes

MW satellite galaxies lie within a thin plane (Pawlowski & Kroupa 2013, 2020). Analogous situation for M31 (Ibata+ 2013)

Galaxies observed forming within tidal tails (Mirabel+ 1992)

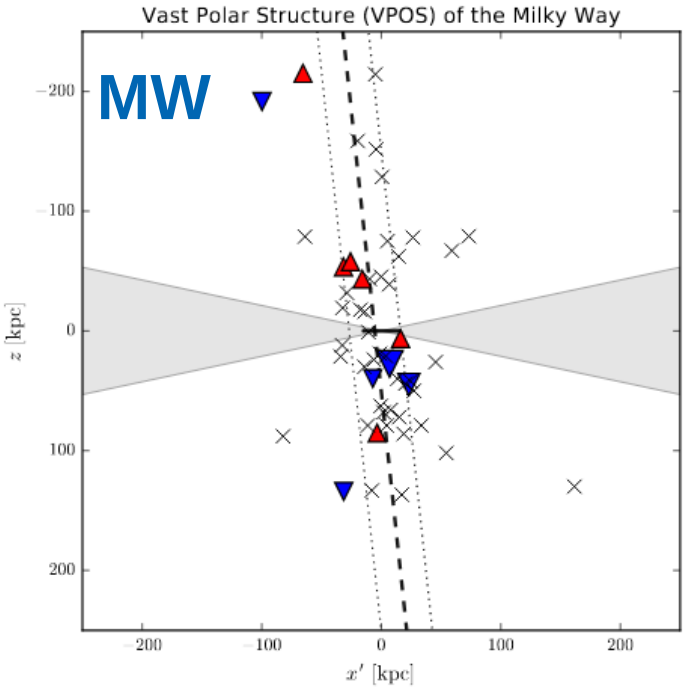

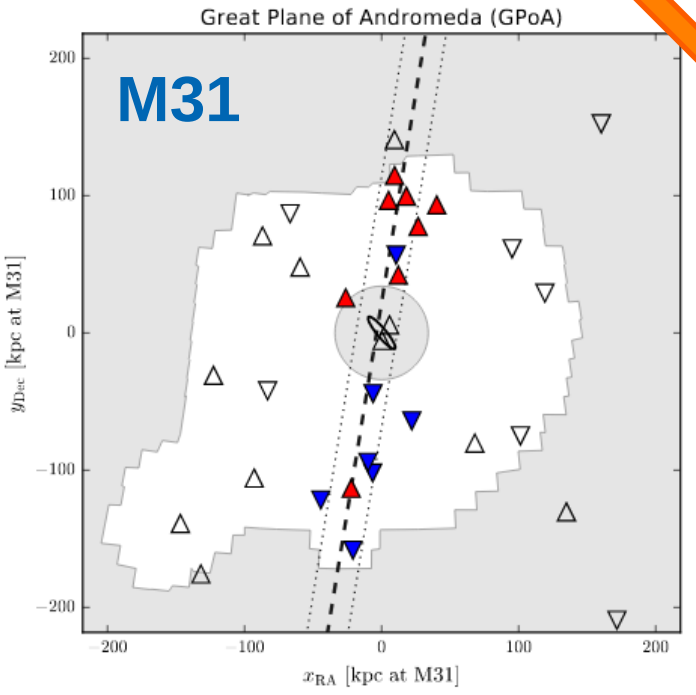

Satellites were formed from tidal debris. Alternatives not very likely (Pawlowski+ 2014, and references therein)

The satellite planes in ΛCDM (Pawlowski 2021)

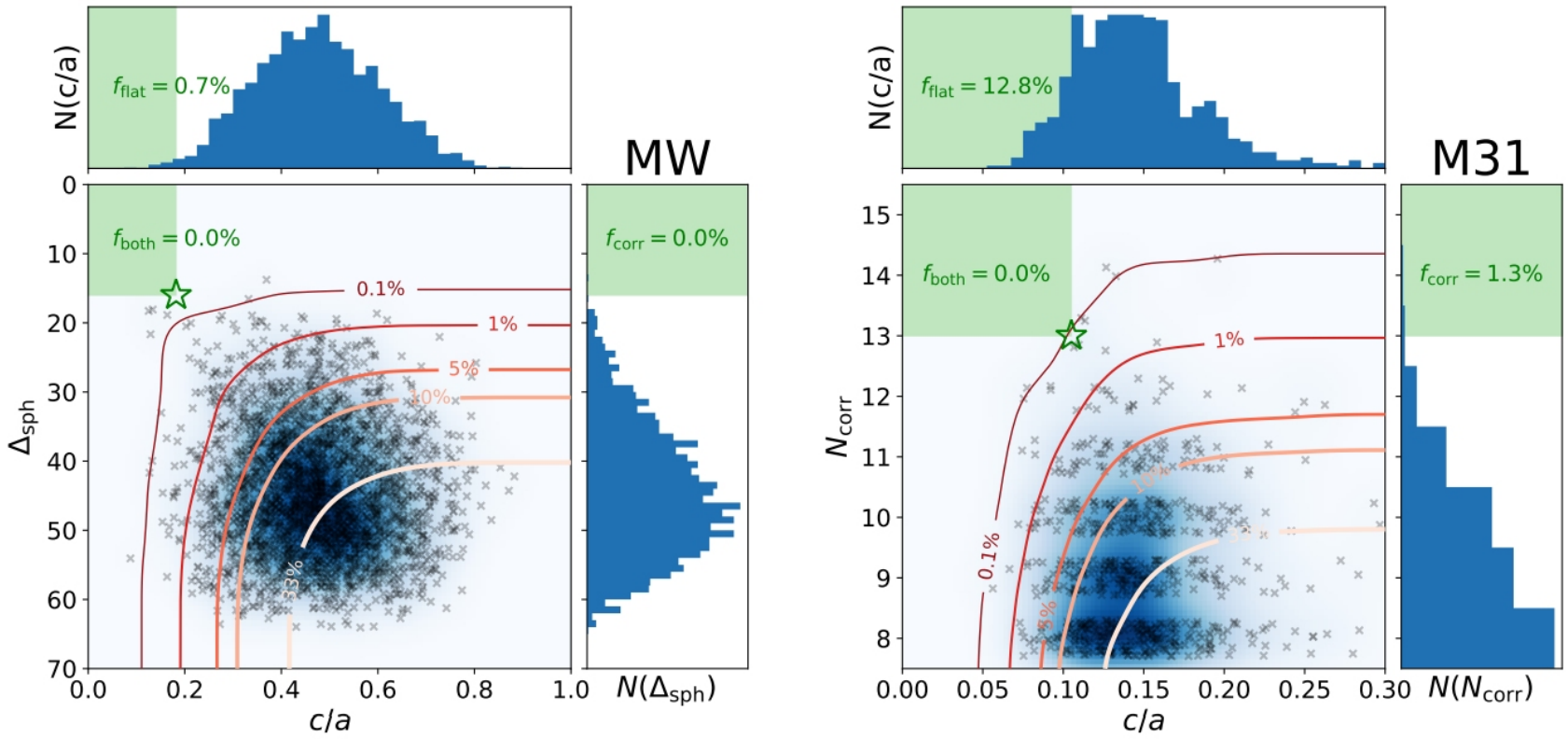

The satellite planes in ΛCDM (Pawlowski 2021)

- **3D distribution of satellites known only in these three cases**
- **Very substantial tension with ΛCDM arises 3/3 times (1/2500 for both MW and M31, 1/500 for Cen A)**
- **Dark matter filaments are as thick as MW/M31 virial radius, but satellite planes 10x thinner**

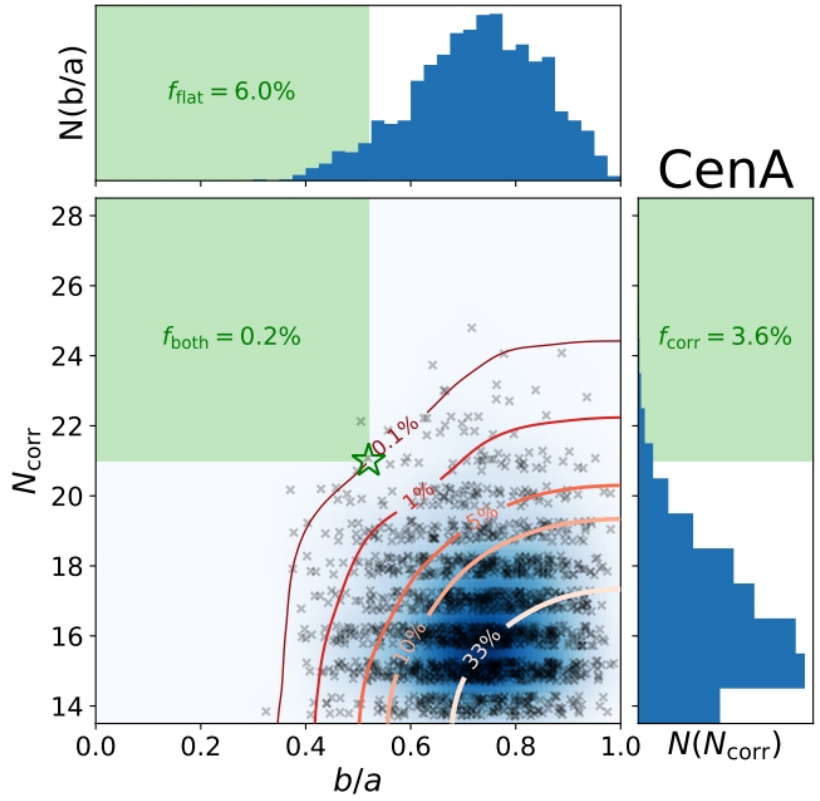

Local Group satellite planes

MW satellite galaxies lie within a thin plane (Pawlowski & Kroupa 2013, 2020). Analogous situation for M31 (Ibata+ 2013)

Galaxies observed forming within tidal tails (Mirabel+ 1992)

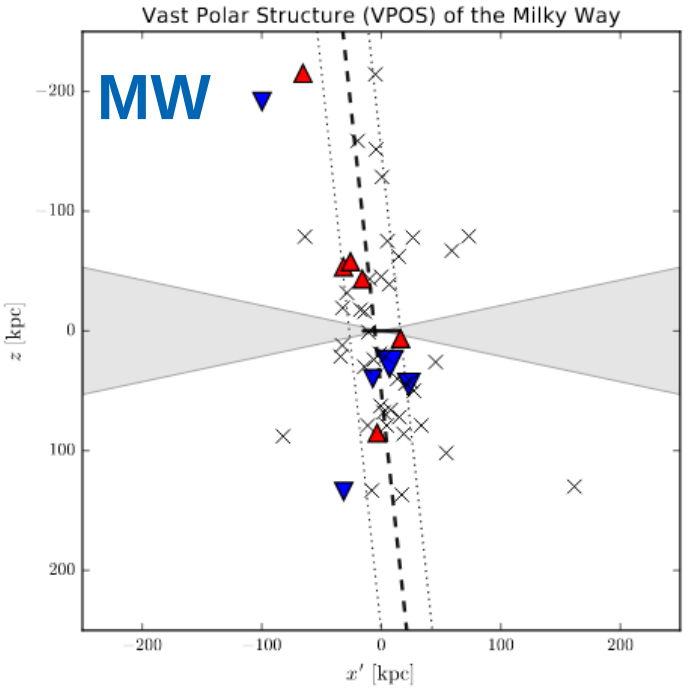

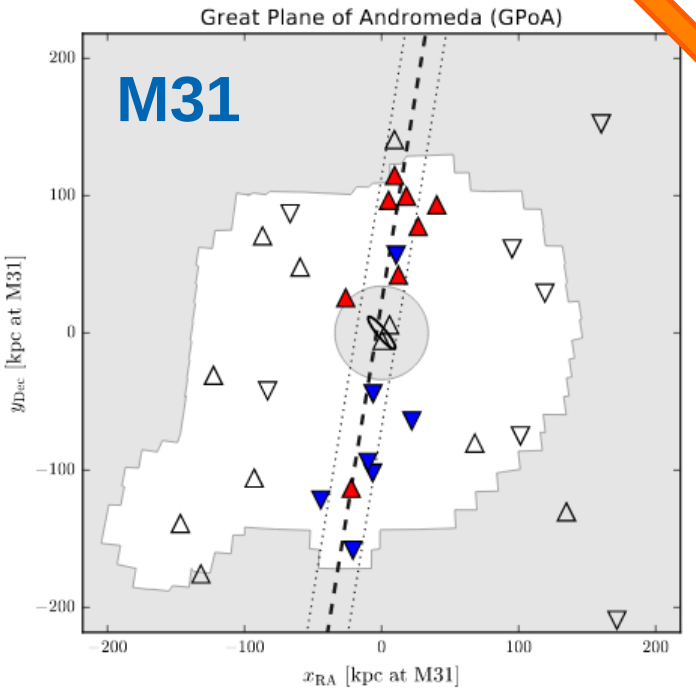

Satellites were formed from tidal debris. Alternatives not very likely (Pawlowski+ 2014, and references therein)

Should only contain baryons as DM can't cool and form dense tidal tails (Wetzstein+ 2007)

Local Group satellite planes

MW satellite galaxies lie within a thin plane (Pawlowski & Kroupa 2013, 2020). Analogous situation for M31 (Ibata+ 2013)

Galaxies observed forming within tidal tails (Mirabel+ 1992)

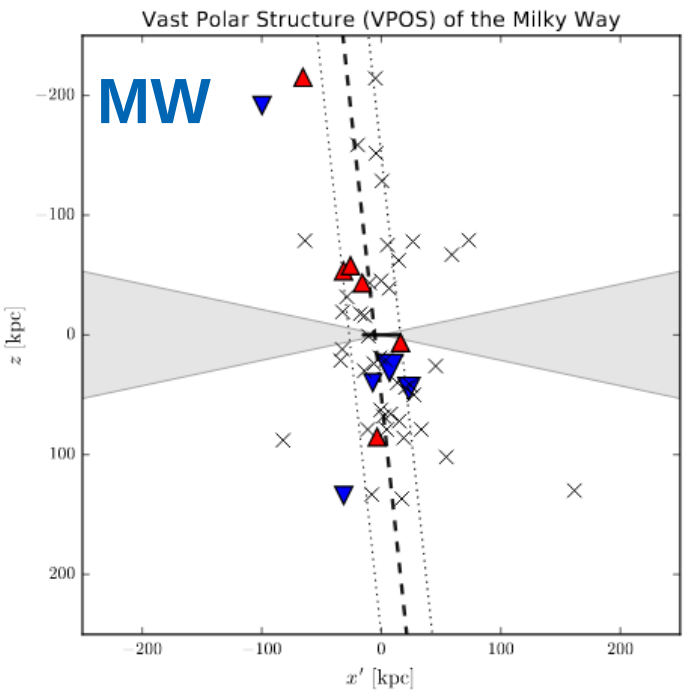

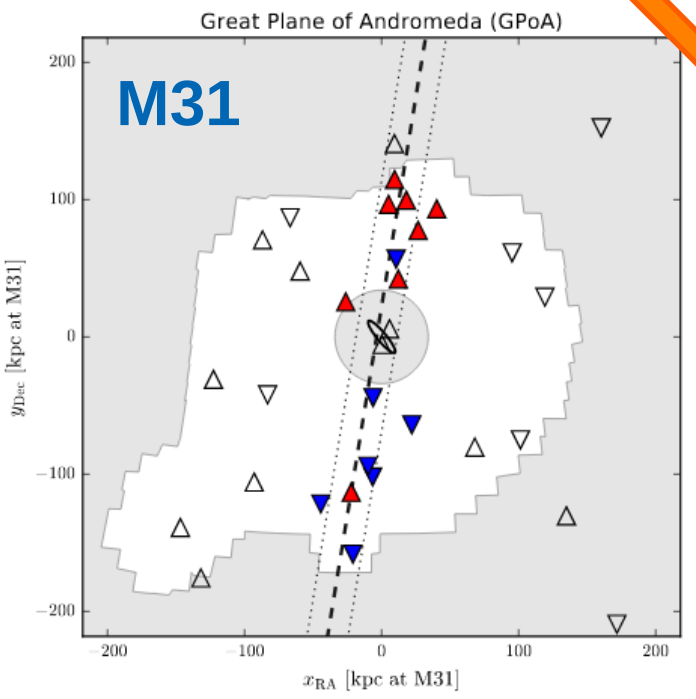

Satellites were formed from tidal debris. Alternatives not very likely (Pawlowski+ 2014, and references therein)

Should only contain baryons as DM can't cool and form dense tidal tails (Wetzstein+ 2007)

MW and M31 satellite galaxies have high internal velocity dispersions, requiring strong self-gravity (McGaugh & Wolf, 2010; McGaugh & Milgrom 2013)

Internal dynamics can't be explained by Newtonian gravity (Kroupa, 2015)

Milgromian dynamics (MOND)

- **Newtonian gravity/GR developed using Solar System constraints**
- **MOND developed by M. Milgrom (1983) to address rotation curves without cold dark matter by going beyond Newton**
- **Lagrangian formalism**
  - Milgrom 2010

$$L = L_K - L_P = \rho\left(\frac{1}{2}v^2 - \Phi\right) - \frac{1}{8\pi G}\left[2\boldsymbol{g}\cdot\boldsymbol{g}_N - a_0^2 f(g_N)\right]$$

Extremize action

- **Non-linear generalization of the Poisson eqn.:**
  - external field effect (EFE, Milgrom 1986)
  - breaks strong equivalence principle (as observed by Chae+ 2020, 2021)

$$\nabla\cdot\boldsymbol{g} = \nabla\cdot\left[\nu\left(\frac{g_N}{a_0}\right)\boldsymbol{g}_N\right], \quad f \Leftrightarrow \nu$$

Milgromian dynamics (MOND)

- **Newtonian gravity/GR developed using Solar System constraints**
- **MOND developed by M. Milgrom (1983) to address rotation curves without cold dark matter by going beyond Newton**
- **Lagrangian formalism**
  - Milgrom 2010

$$L = L_K - L_P = \rho\left(\frac{1}{2}v^2 - \Phi\right) - \frac{1}{8\pi G}\left[2\boldsymbol{g}\cdot\boldsymbol{g}_N - a_0^2 f(g_N)\right]$$

Extremize action

- **Non-linear generalization of the Poisson eqn.:**
  - external field effect (EFE, Milgrom 1986)
  - breaks strong equivalence principle (as observed by Chae+ 2020, 2021)

$$\nabla\cdot\boldsymbol{g} = \nabla\cdot\left[\nu\left(\frac{g_N}{a_0}\right)\boldsymbol{g}_N\right], \quad f \Leftrightarrow \nu$$

- **Milgrom's constant (from RAR):** $a_0 = 1.2\times10^{-10} m/s^2$
- **Asymptotic limits in spherical symmetry:**

$$g_N \ll a_0:\ g = \sqrt{a_0 g_N}, \quad g_N \gg a_0:\ g = g_N$$

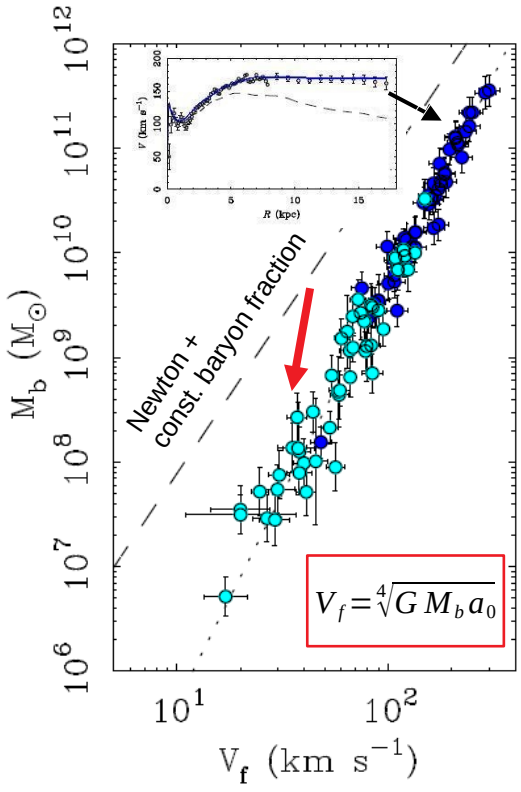

Milgromian dynamics (MOND)

- **Newtonian gravity/GR developed using Solar System constraints**
- **MOND developed by M. Milgrom (1983) to address rotation curves without cold dark matter by going beyond Newton**
- **Lagrangian formalism**
  - Milgrom 2010

$$L = L_K - L_P = \rho\left(\frac{1}{2}v^2 - \Phi\right) - \frac{1}{8\pi G}\left[2\boldsymbol{g}\cdot\boldsymbol{g}_N - a_0^2 f(g_N)\right]$$

Extremize action

- **Non-linear generalization of the Poisson eqn.:**

$$\nabla\cdot\boldsymbol{g} = \nabla\cdot\left[\nu\left(\frac{g_N}{a_0}\right)\boldsymbol{g}_N\right], \quad f \Leftrightarrow \nu$$

  - external field effect (EFE, Milgrom 1986)
  - breaks strong equivalence principle (as observed by Chae+ 2020, 2021)
- **Milgrom's constant (from RAR):** $a_0 = 1.2\times10^{-10} m/s^2$
- **Asymptotic limits in spherical symmetry:**

$$g_N \ll a_0:\ g = \sqrt{a_0 g_N}, \quad g_N \gg a_0:\ g = g_N$$

- **Relativistic MOND theory where gravitational waves travel at *c* (Skordis & Zlosnik 2019, 2021, PRL) and GR-like light deflection**

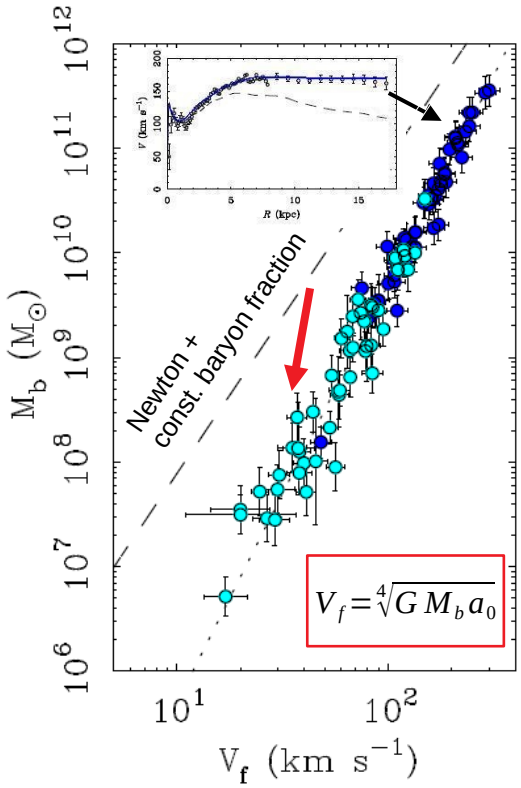

Weak lensing by galaxies

- Galaxy-galaxy weak lensing results also follow the RAR traced by rotation curves
- MOND has GR-like relation between $\boldsymbol{g}$ and light deflection

$$\Delta \hat{\boldsymbol{n}} = \int \frac{2\boldsymbol{g}}{c^2} dl$$

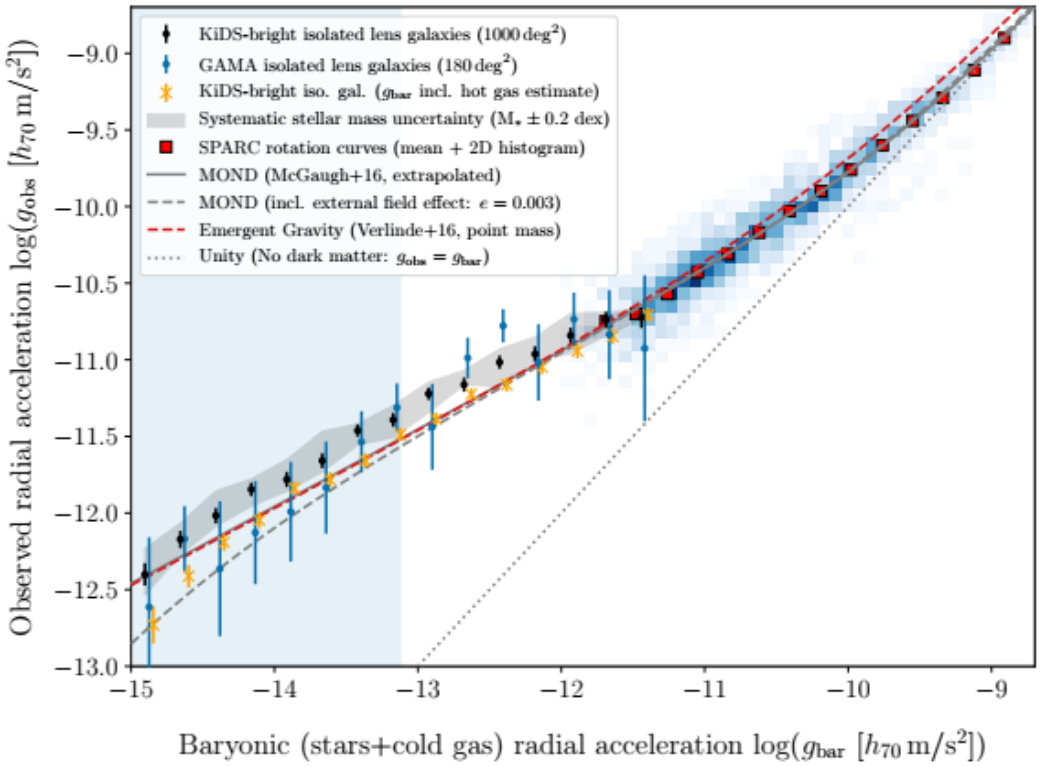

Brouwer+ 2021

Dark matter can fit anything

- **Unwary astronomers were given a rotation curve & image and asked to fit the curve**

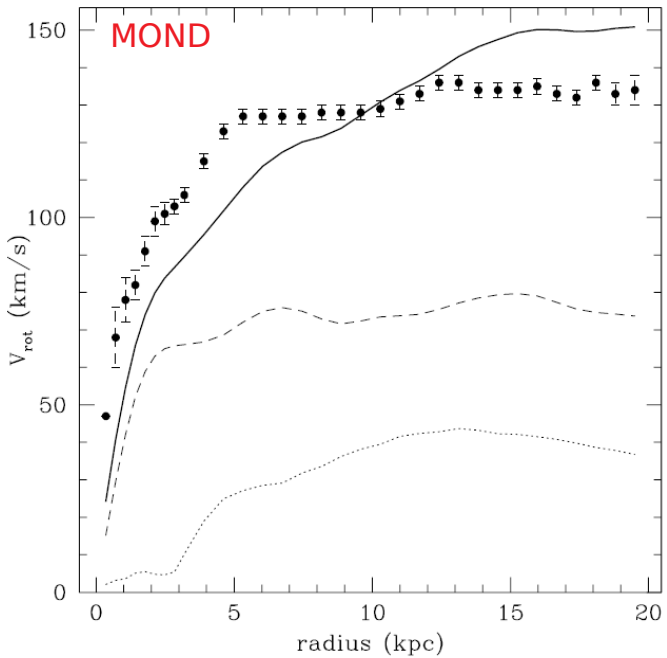

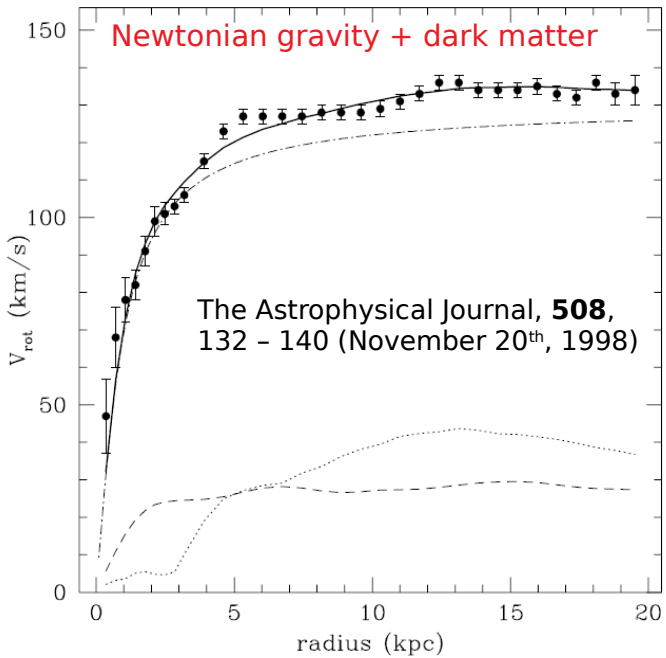

Dark matter can fit anything

- **Unwary astronomers were given a rotation curve & image and asked to fit the curve**
- **Catch: the image was of the wrong galaxy...**

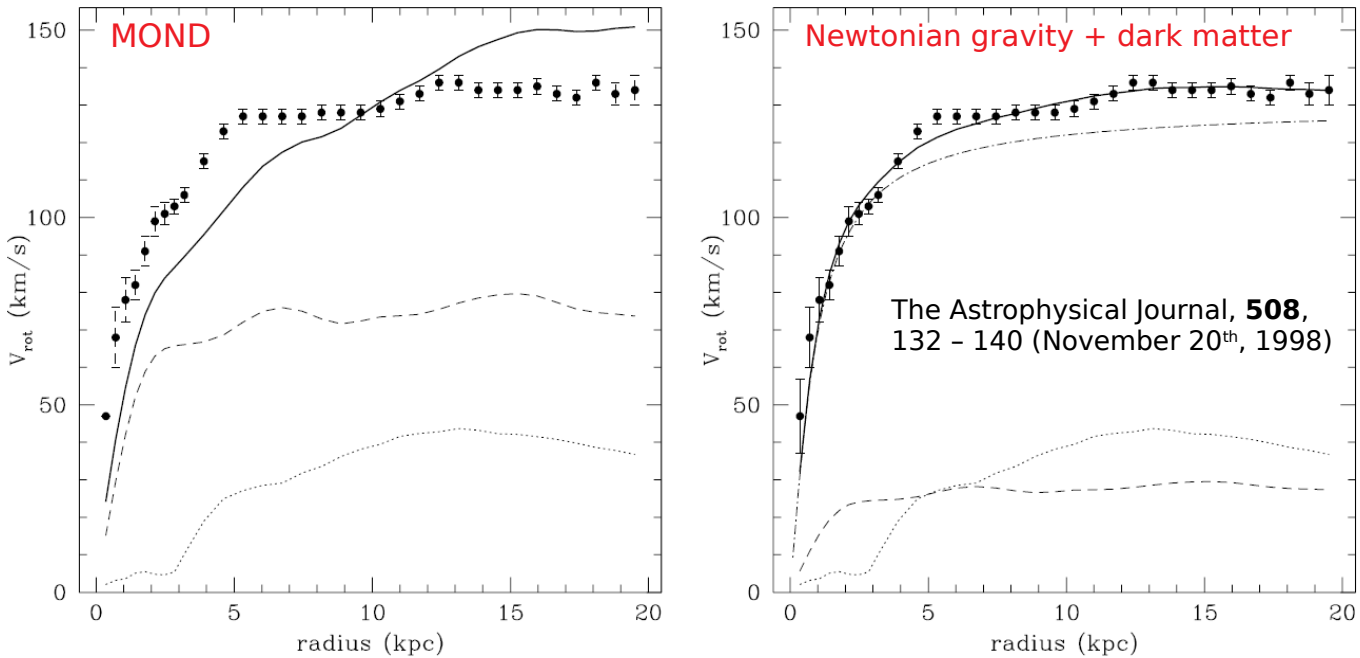

Detection of external field effect (EFE)

- **No EFE expected because galaxies isolated**
- **Isolated galaxies should (and do) have flat outer rotation curves**
  - No EFE required in rotation curve fits ($|\Delta BIC| < 10$)

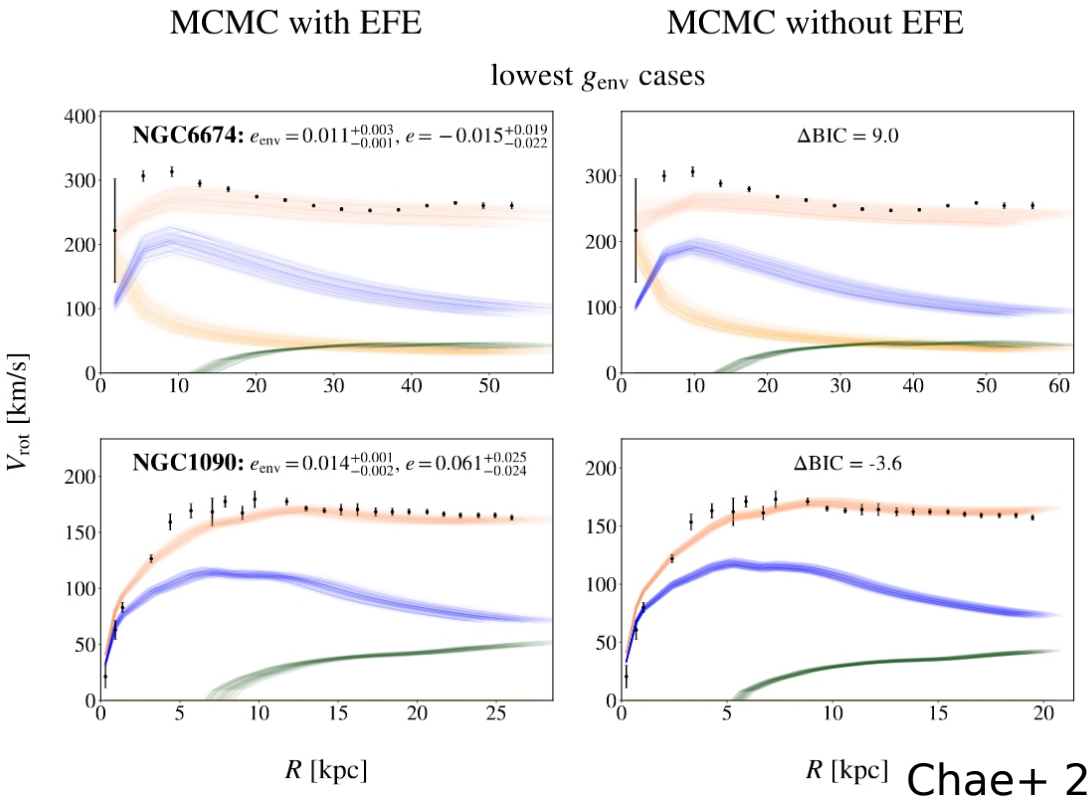

Chae+ 2020

Detection of external field effect (EFE)

- **Strong EFE expected based on environment**
- **Outer rotation curve should be declining**
- **“Very strong” evidence for EFE in rotation curves (ΔBIC >> 10)**
- **Inferred g_{ext} from rotation curve agrees with prior estimates**
- **Similar results in Chae+ 2021**

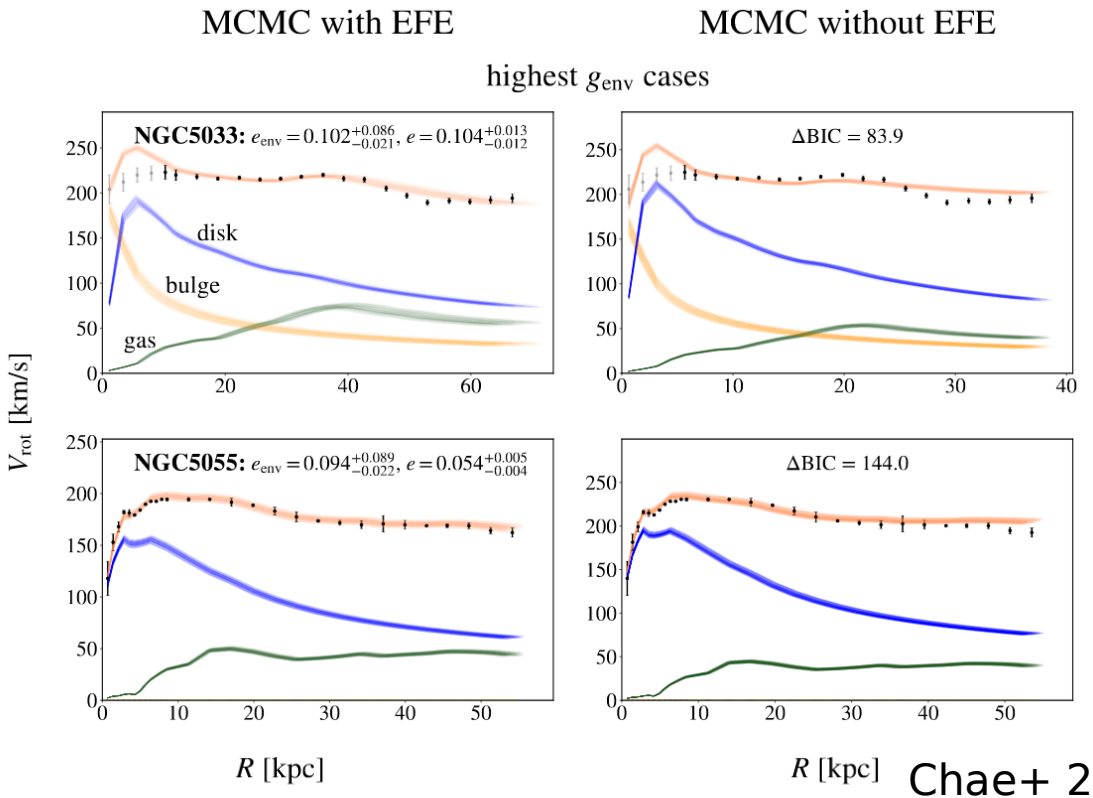

Chae+ 2020

Galaxy bars in different gravity theories

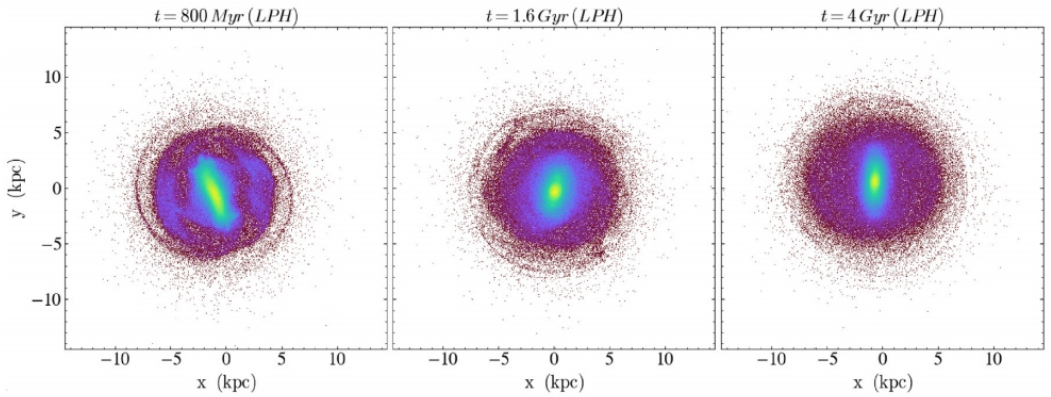

- **Without dominant dark halo, bar pattern speed Ω_p remains constant**
- **Bar slows down only inside live halo due to dynamical friction**

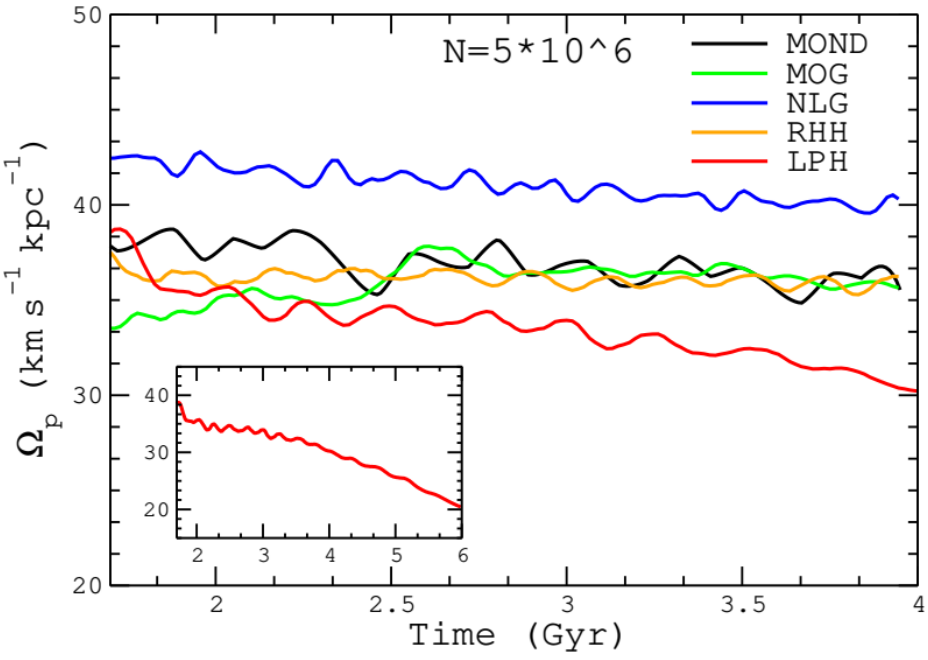

Roshan+ 2021a

Galaxy bars in different gravity theories

- **Quantify speed using $\mathcal{R} \equiv R_{CR}/R_{bar}$,**
  - R_{CR}: corotation radius of bar
  - R_{bar}: bar semi-major axis
- **For almost linear inner rotation curve, reducing Ω_p significantly raises R_{CR}**
- **$\mathcal{R}$ = 1 – 1.4: fast bar**
- **$\mathcal{R}$ > 1.4: slow bar**
- **$\mathcal{R}$ < 1: see Cuomo+ 2021**

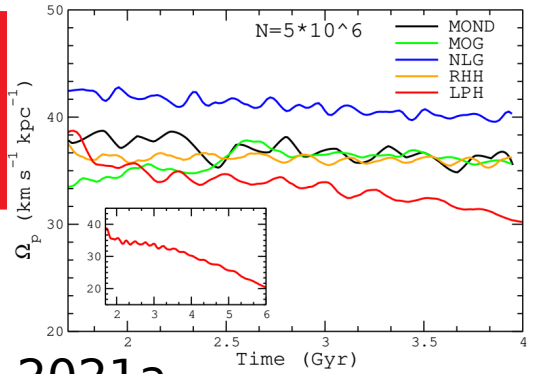

Roshan+ 2021a

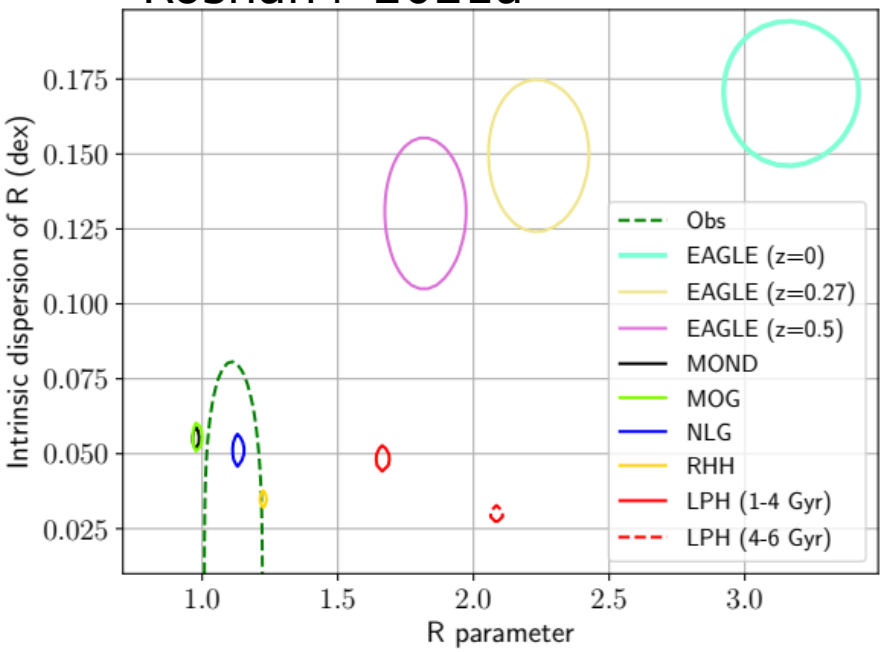

Galaxy bars

Simulation	Sample size	Tension
TNG50	209	12.62σ
TNG100	745	13.56σ
EAGLE100	70	9.69σ

- **42 galaxies with direct $\mathcal{R}$ measurements from Cuomo+ 2020**
- **ΛCDM results are converged**
- **Level of tension related to sample size**
- **Bars evolve little over time (Lee+ 2022)**

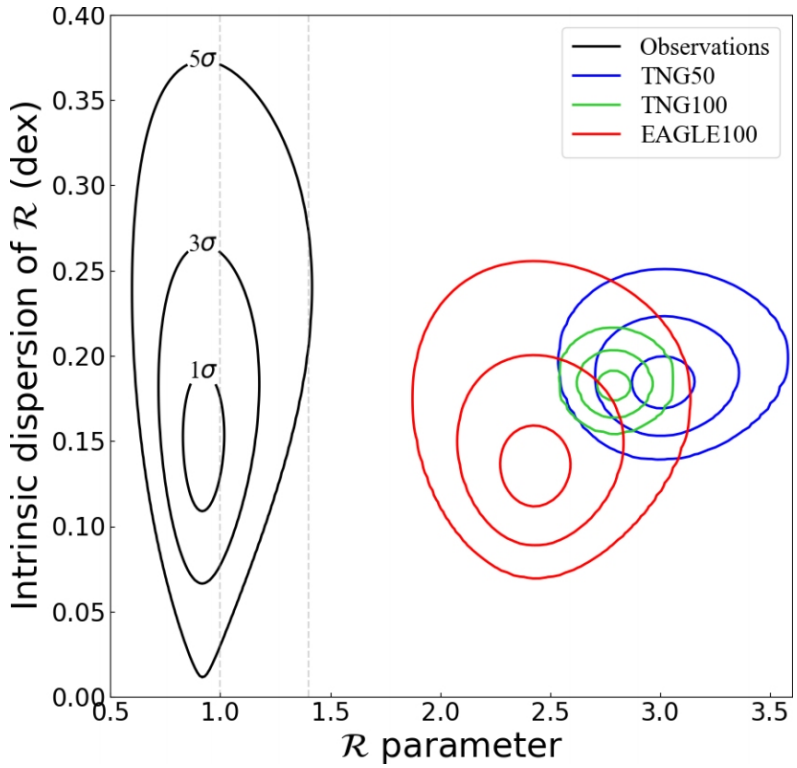

Roshan+ 2021b

Superfluid dark matter & Emergent gravity

Both theories reduce to MOND in galaxies, but specify the interpolating function

Sum rule: $\nu = 1 + \sqrt{\frac{a_0}{g_N}}$

Empirical fit

MLS: $\nu = \frac{1}{1-\exp\left(-\sqrt{\frac{g_N}{a_0}}\right)}$

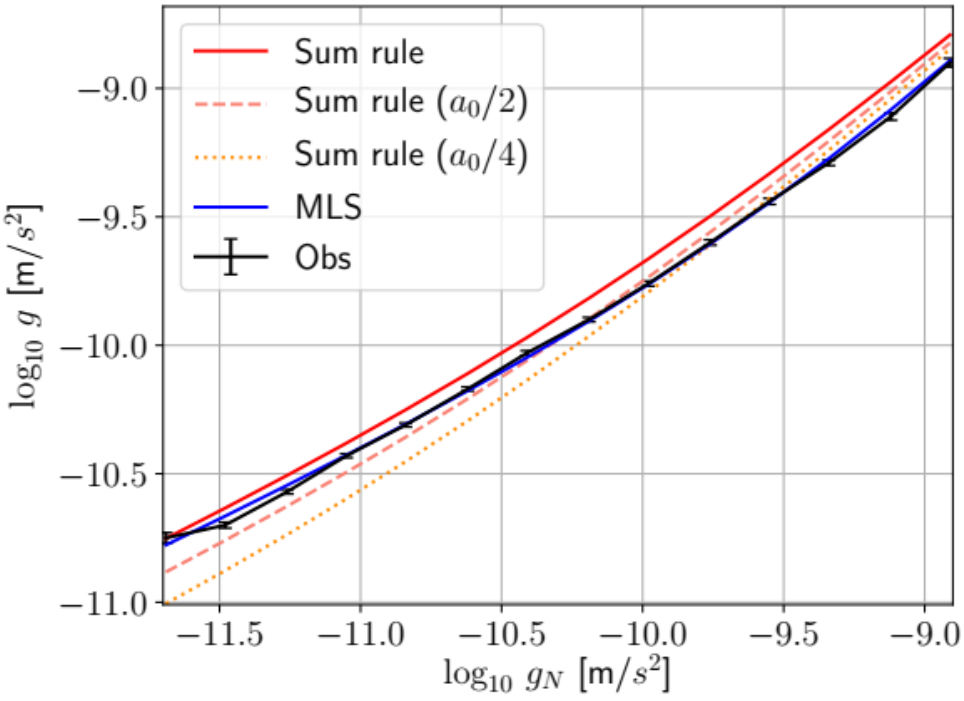

Credit: Elena Asencio

Superfluid dark matter & Emergent gravity

- **Sum rule incompatible with observed RAR for any a_0**
- **Superfluid dark matter in tension with rotation curves and lacks natural explanation for why they show the same RAR as lensing data (Mistele, McGaugh & Hossenfelder, ArXiv: 2201.07282)**

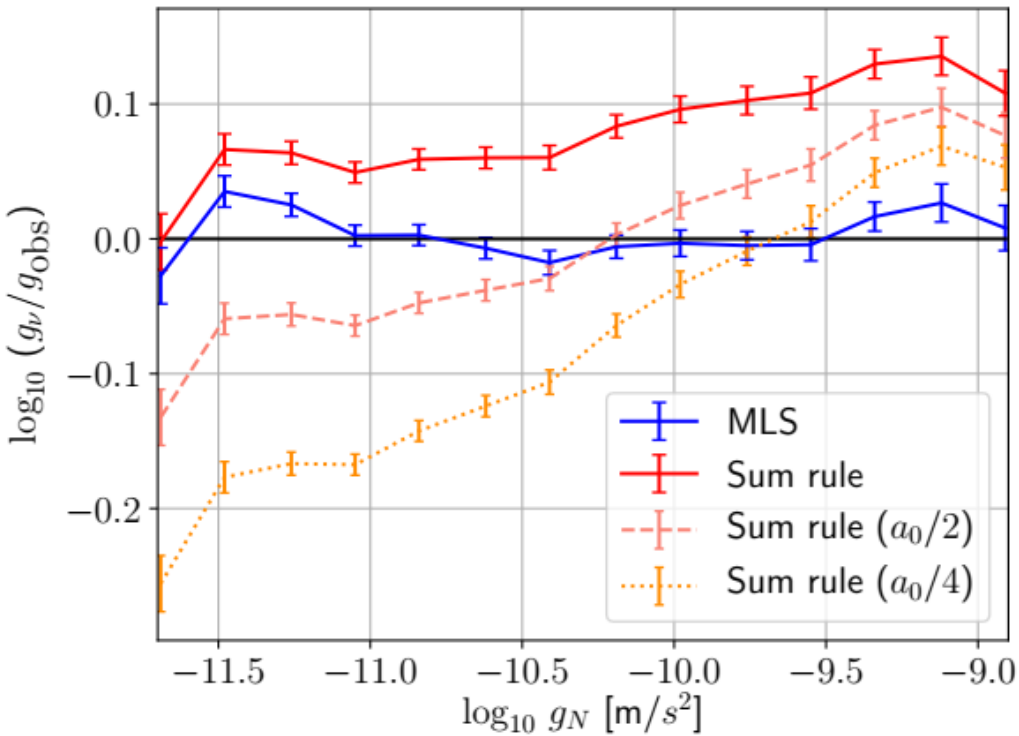

Credit: Elena Asencio

Cosmology

Cosmological MOND framework (vHDM): overview

- **Proposed by Angus 2009 (MNRAS, 394, 527)**
- **Cold dark matter (CDM) replaced by**
  diffuse collisionless matter
  - e.g. 11 eV/c^2 sterile neutrinos (e.g. Angus+2007)
  - same overall mass-energy budget as in ΛCDM
- **Standard background cosmology *a(t)***
  → Nucleosynthesis (BBN)
  - e.g. Skordis 2006 (Phys. Rev. D, 74, 103513)
- **MOND is applied only to perturbations**
  - e.g. Nusser 2002, Llinares+ 2008, Angus+ 2013, Katz+ 2013, Candlish 2016
- **External field effect from surrounding structures**
  - consequence of the non-linearity of MOND (e.g. Banik+ 2018, ArXiv1808.10545)

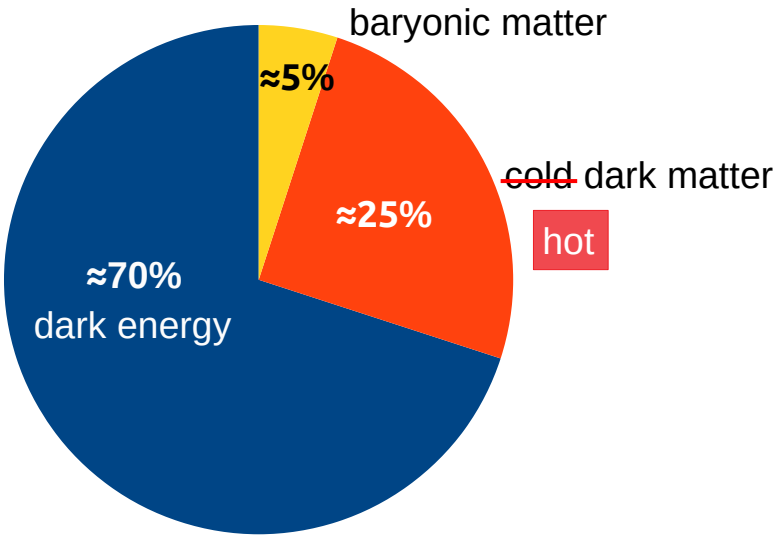

vHDM framework: impact on CMB

- **Standard expansion history**

  → same angular diameter distance to CMB
- **MOND is sub-dominant at time of recombination**

  (z = 1100) because g ≈ 20 a_0
- **Free streaming effects negligible if $m_\nu > 10$ eV/c²**

> We impose a prior on the physical thermal mass, $m^{\rm thermal}_{\rm sterile} < 10$ eV, when generating parameter chains, to exclude regions of parameter space in which the particles are so massive that their effect on the CMB spectra is identical to that of cold dark matter.

Planck Collaboration XIII (2016), section 6.4.3

- **MOND effects become important only at z < 50**

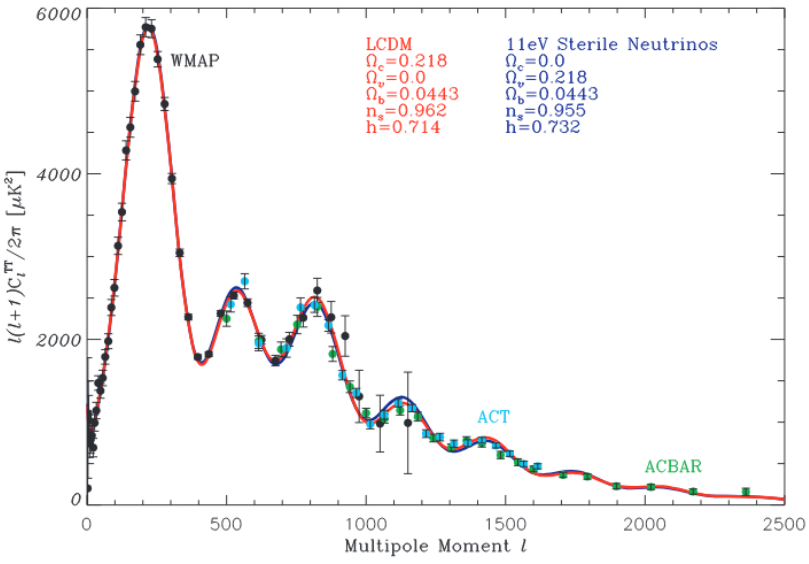

Angus & Diaferio 2011

Astronomical evidence for extra collisionless matter

- **Offset X-ray and weak lensing peaks**
- **$g > a_0$: MOND effects small**

  → Collisionless matter required
- **Tremaine-Gunn limit: $m_\nu > 2$ eV/c² (Angus+ 2007, ApJ, 654, L13)**
- **30 virialized galaxy clusters well fit with 11 eV/c² sterile neutrinos (Angus+ 2010)**
- **CMB constraints imply collisionless particle mass >10 eV/c²**

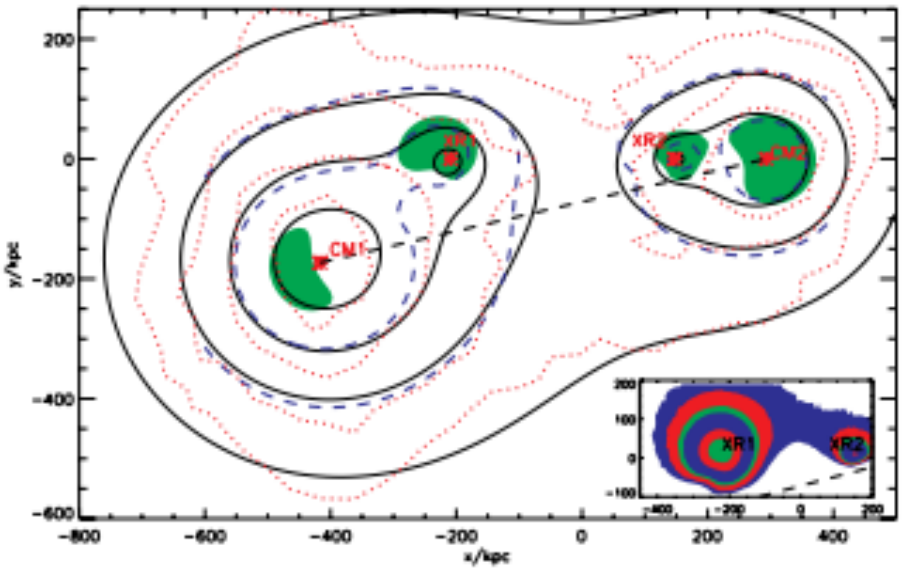

MOND fit to Bullet Cluster (Angus+ 2007)

Hierarchical structure formation

Density fluctuations

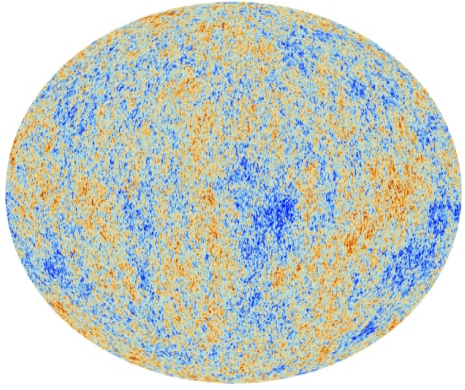

Cosmic microwave background seen by Planck 2013. Copyright: ESA, Planck Collaboration

Small structures (e.g., stars)

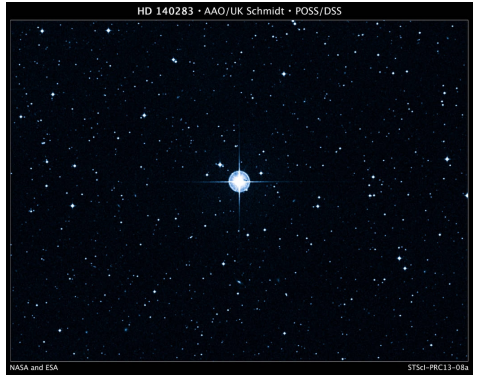

Star HD 140283. Credit: Digitized Sky Survey (DSS), STScI/AURA, Palomar/Caltech, and UKSTU/AAO

Large structures (e.g., galaxies)

Spiral Galaxy M81.Image credit: X-ray: NASA/CXC/SAO; Optical: Detlef Hartmann; Infrared: NASA/JPL-Caltech

The largest structures: galaxy clusters

Galaxy cluster Abell 1689. Credit: NASA, ESA, the Hubble Heritage Team (STScI/AURA), J. Blakeslee (NRC Herzberg Astrophysics Program, Dominion Astrophysical Observatory), and H. Ford (JHU)

If the cosmological model is correct, it should statistically predict when these formed

In recent years, surveys found...

SPT-CL J2106-5844

- $z = 1.13$
- Mass $\simeq 1 \times 10^{15}\ M_{\odot}$

ACT-CL J0102-4915 (El Gordo)

- $z = 0.87$
- Mass $\simeq 3 \times 10^{15}\ M_{\odot}$
- $V_{infall} \simeq 2500$ km/s

1E 0657-56 (Bullet Cluster)

- $z = 0.30$
- Mass $\simeq 2.2 \times 10^{14}\ M_{\odot}$
- $V_{infall} \simeq 3000$ km/s

PLCK G287.0+32.9

- $z = 0.39$
- Mass $\simeq 2 \times 10^{15}\ M_{\odot}$

...and more

ΛCDM predicts that galaxy clusters at $z \simeq 1$ should have a maximum mass of $M \simeq 1.7 \times 10^{15}\ M_{\odot}$, so objects with a similar mass should be extremely rare.

But...
$M_{El\ Gordo} \simeq 3 \times 10^{15}\ M_{\odot}$ at z = 0.87!!

El Gordo (ACT-CL J0102-4915)

- Redshift: $z = 0.87$ (more than 7 billion light years from Earth)
- Two subclusters of total mass $M_{200} \simeq 3 \times 10^{15} M_{\odot}$ (see also Kim+ 2021) and mass ratio of 3.6
- Infall velocity: $V_{infall} \simeq 2500$ km/s (1.24x its escape velocity)
- Most X-ray luminous, and brightest Sunyaev-Zel'dovich (SZ) effect galaxy cluster at this redshift.
- X-ray emission morphology: single peak and two faint tails.

El Gordo in X-ray light from NASA's Chandra X-ray Observatory in blue, along with optical data from the European Southern Observatory's Very Large Telescope (VLT) in red, green, and blue, and infrared emission from the NASA's Spitzer Space Telescope in red and orange. Credits: X-ray: NASA/CXC/Rutgers/J. Hughes et al; Optical: ESO/VLT & SOAR/Rutgers/F. Menanteau; IR: NASA/JPL/Rutgers/F. Menanteau.

El Gordo galaxy cluster interaction

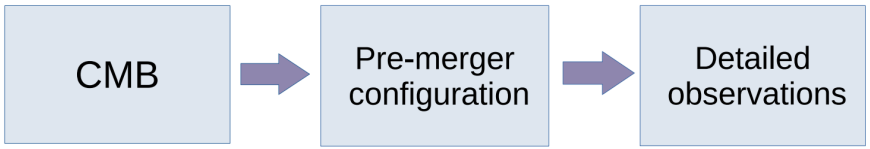

Cosmological simulations (Jubilee simulation, Watson+ 2014)

Hydrodynamical simulations (Zhang+ 2015)

- **Mass-redshift distribution of fast-interacting clusters along past lightcone in ΛCDM simulation**
  - $\widetilde{M} \equiv \log_{10} \frac{M_{total}}{M_{\odot}}$
  - $a \equiv \frac{1}{1+z}$
- **El Gordo inconsistent at 6.16σ (P = 7.51e-10, solid red contour)**

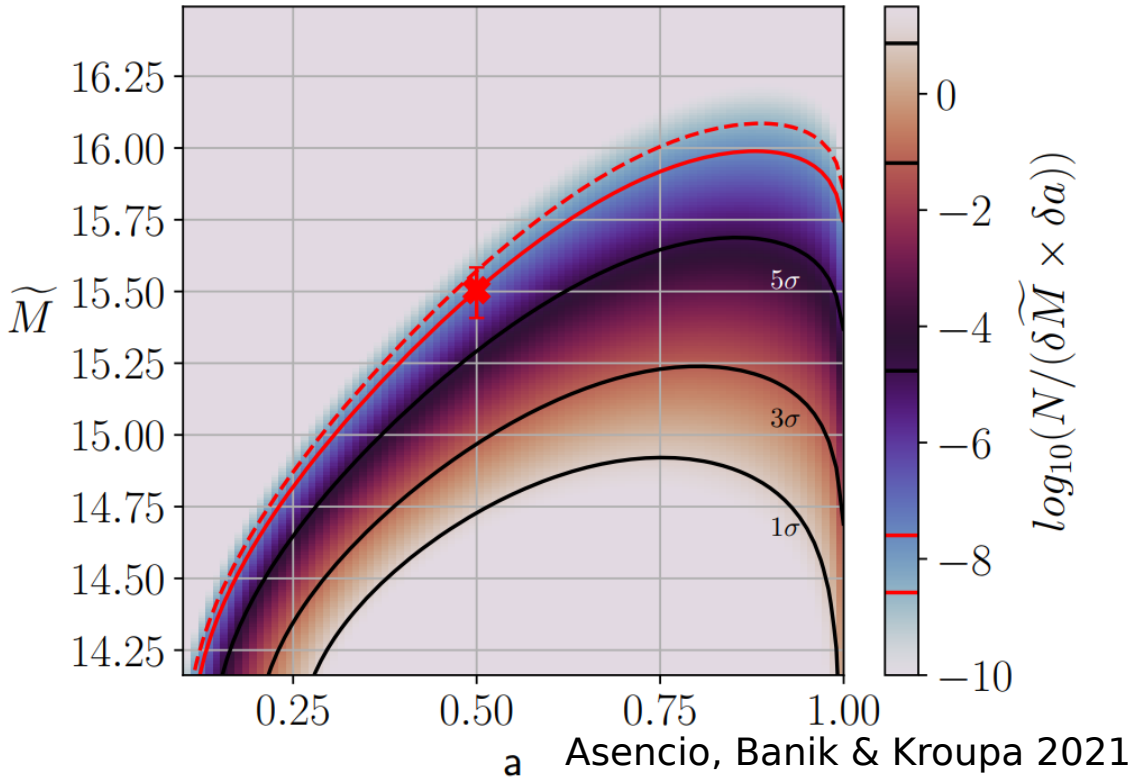

Asencio, Banik & Kroupa 2021 (MNRAS, 500, 5249)

The Keenan-Barger-Cowie (KBC) void

- **A local underdensity is evident across the entire electromagnetic spectrum, ranging from radio to X-ray**
  - Optical: Maddox+1990, Zucca+1997
  - Radio: Rubart & Schwarz 2013, Rubart, Bacon & Schwarz 2014, Secrest+ 2020
  - X-ray: Böhringer+2015, Böhringer, Chan, Collins 2020
- **NIR: Keenan, Barger, Cowie 2013, ApJ, 775, 62**
  - 2M++ galaxy catalog with spectroscopic redshifts
  - void evident in number counts (luminosity function)
  - density about **0.5x cosmic mean** between **40 – 300 Mpc** over 90% of the sky (see also Wong+ 2022)

$$\delta_{obs} \equiv 1-\frac{\rho}{\rho_0} \approx 0.46 \pm 0.06$$

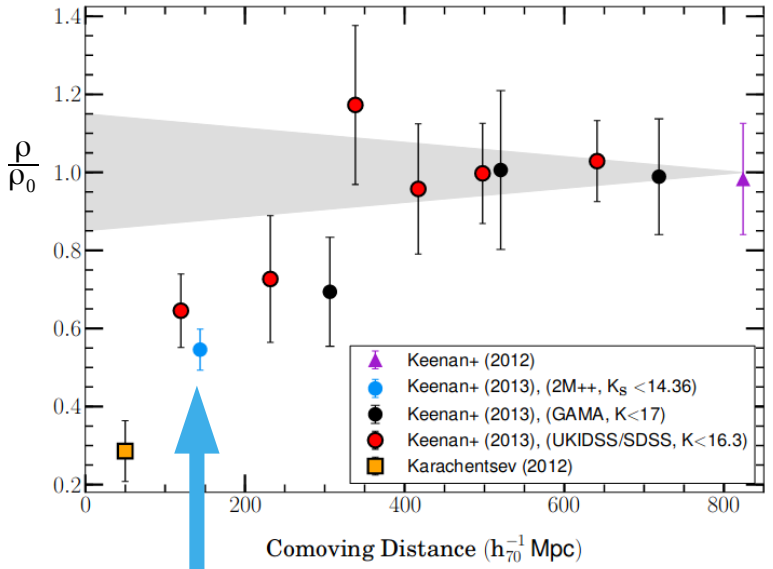

Credits: Kroupa (2015)

Keenan+ (2013): 2M++ with $K_s < 14.36$

KBC 2013, ApJ, 775, 62: density profile

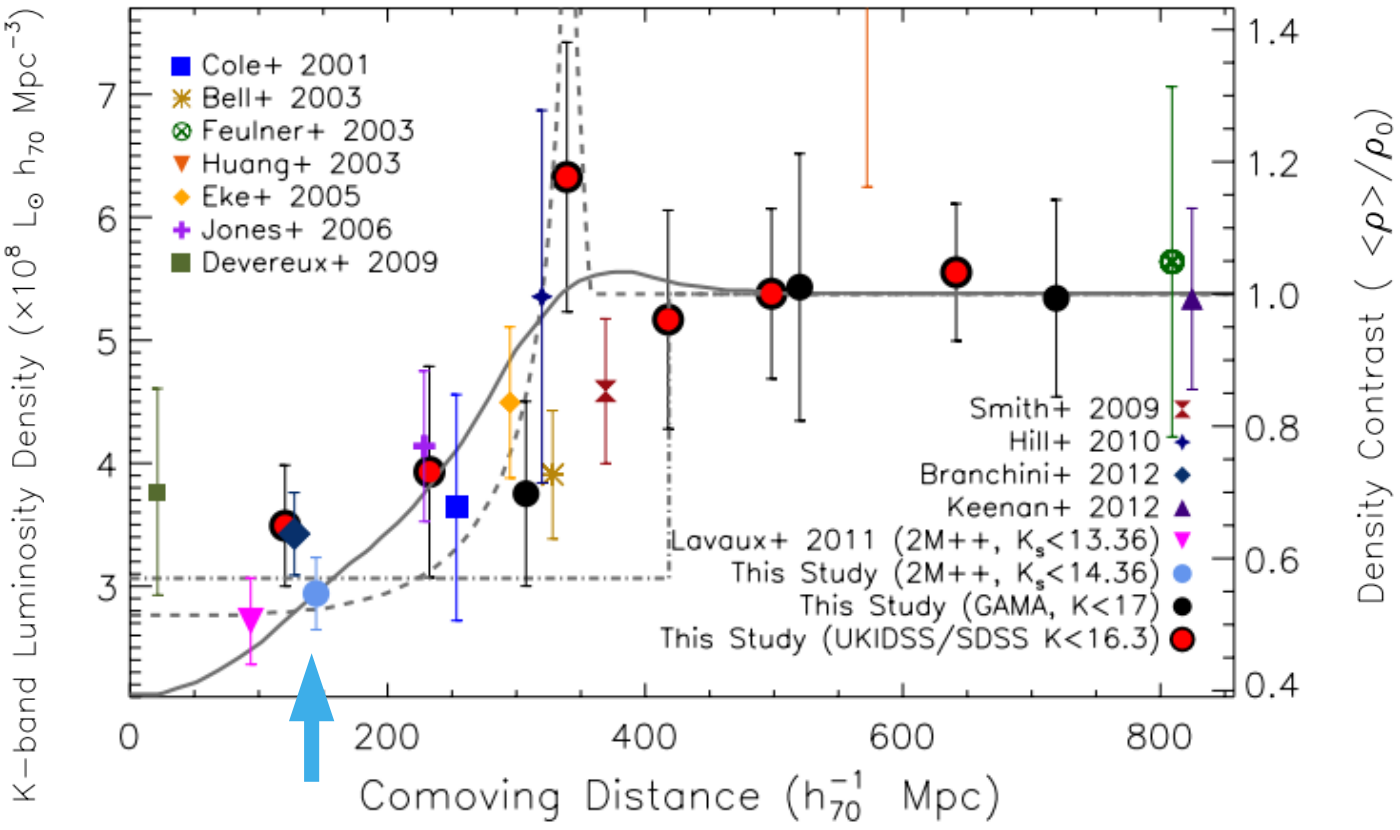

The KBC void and Hubble tension in ΛCDM

Spheres with an inner radius of 40 Mpc and an outer radius of 300 Mpc

Haslbauer, Banik & Kroupa 2020 (MNRAS, 499, 2845)

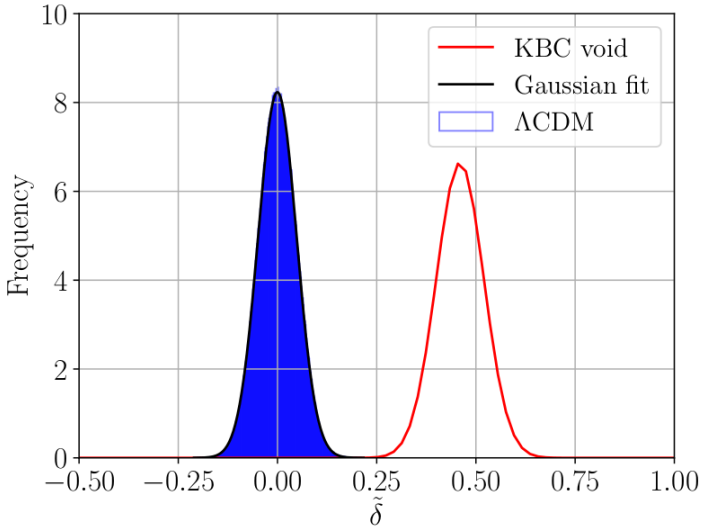

Allowance made for redshift space distortion (RSD): Higher local *H*

The KBC void falsifies ΛCDM at 6.04σ

The KBC void and Hubble tension in ΛCDM

Spheres with an inner radius of 40 Mpc and an outer radius of 300 Mpc

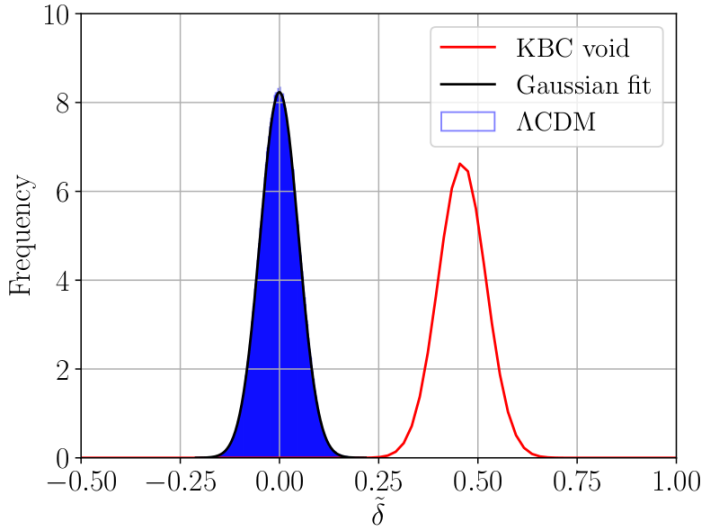

Allowance made for redshift space distortion (RSD): Higher local *H*

Haslbauer, Banik & Kroupa 2020 (MNRAS, 499, 2845)

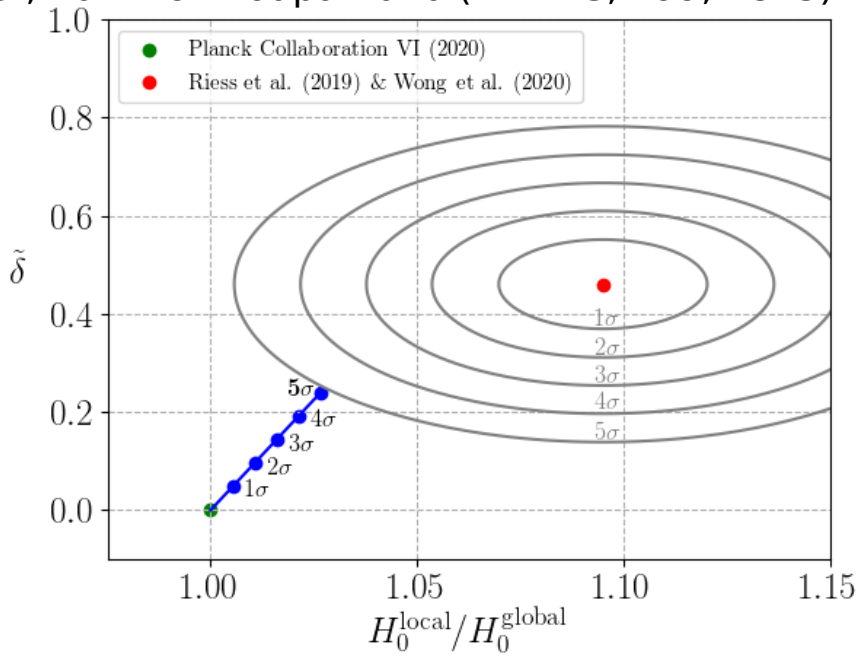

The KBC void falsifies ΛCDM at 6.04σ

Combined, the KBC void + Hubble tension falsify ΛCDM at 7.09σ

Void evident from supernovae alone

- **preferred parameters very similar to that of the KBC void (RSD-corrected)**

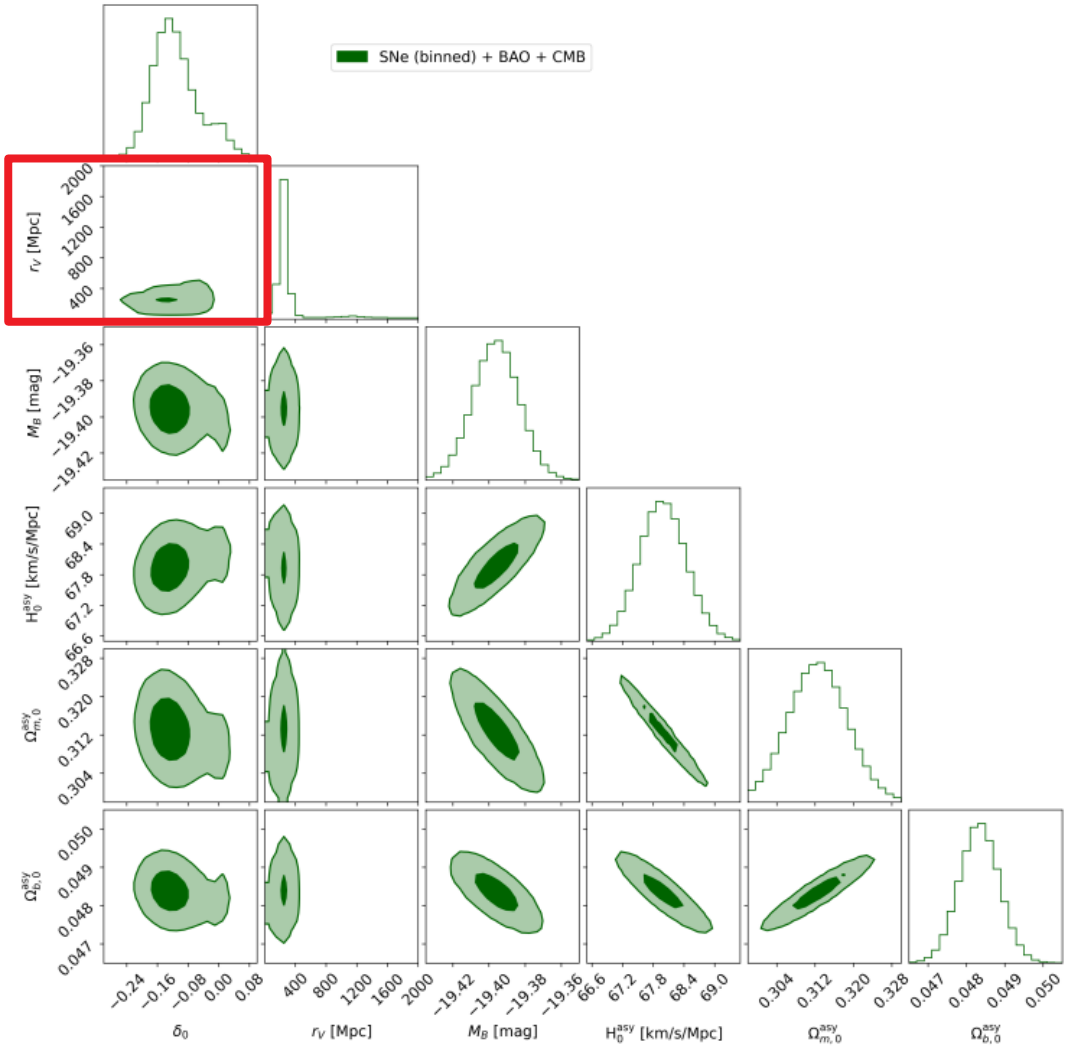

Castello+ 2021 (Arxiv: 2110.04226)

The KBC void and Hubble tension in MOND

- Standard expansion history & overall mass budget

  (CDM → light sterile neutrinos)
- MOND applied only to density perturbations

  e.g. Nusser 2002, Llinares+ 2008, Angus+ 2013, Katz+ 2013, Candlish 2016
- **Semi-analytic model starting from z = 9**
- **Initial Maxwell-Boltzmann underdensity profile**
  - amplitude consistent with CMB
- **External field effect from large scale structure (Milgrom 1986)**
  - gravity from beyond the void

    ⇒ void as a whole moves

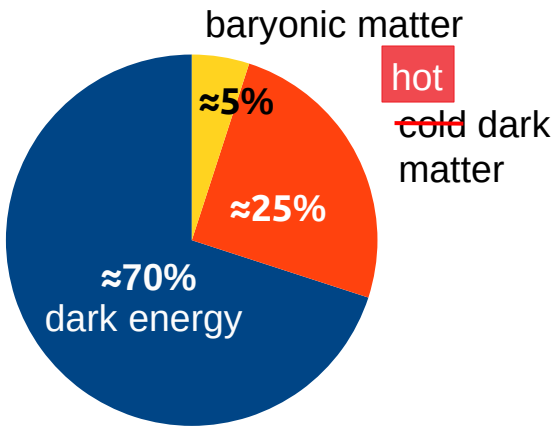

Growth of structure

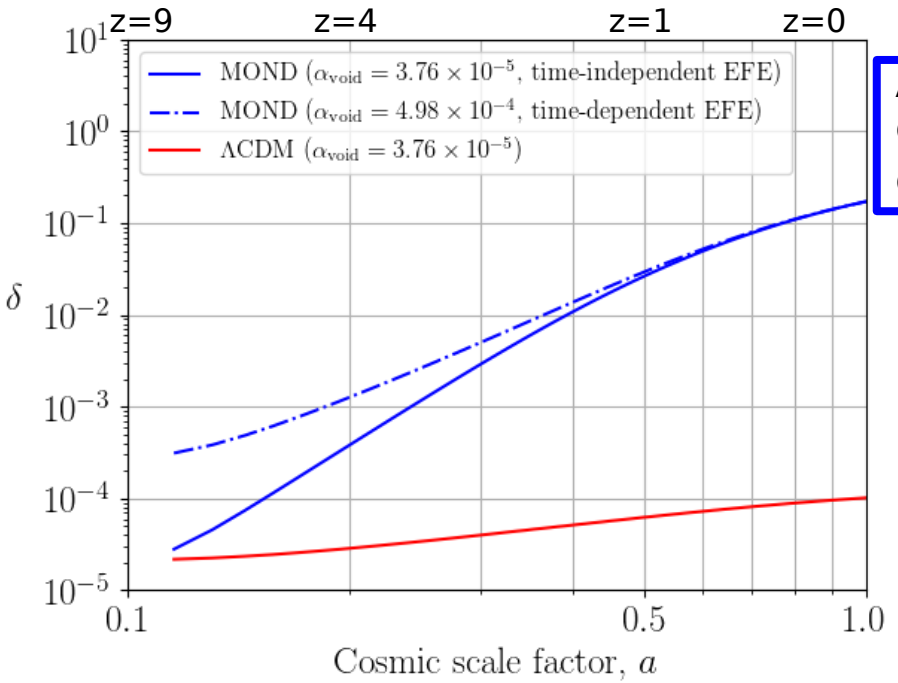

At 300 Mpc:
$g = 0.1a_0$
$g_{ext} = 0.055a_0$

Redshift space distortion (RSD) correction applied

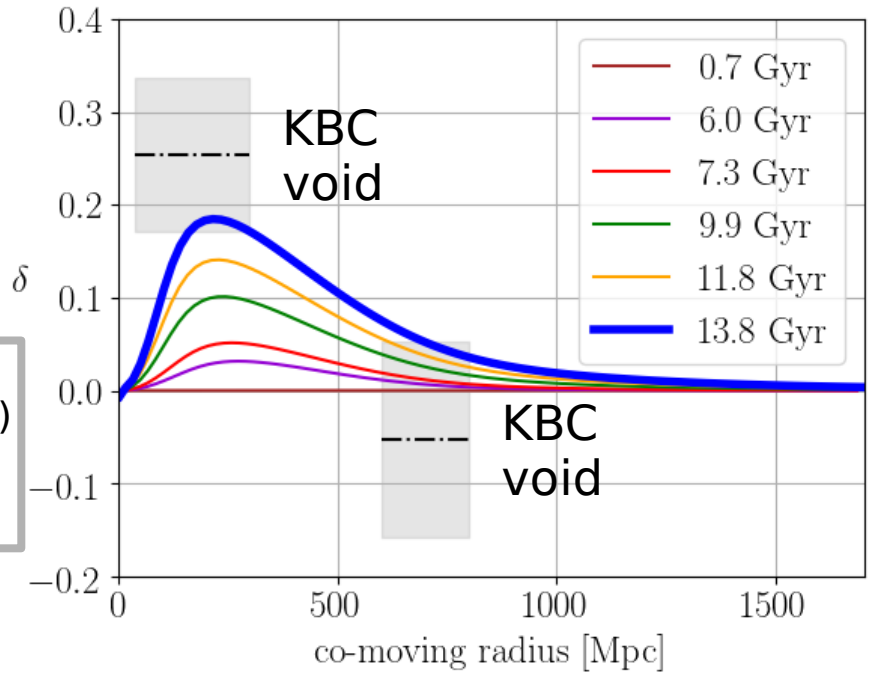

300 cMpc sphere

Haslbauer, Banik & Kroupa 2020 (MNRAS, 499, 2845)

Local Hubble diagram

- **Effects of a local void on cosmological parameters:**
  - local expansion rate is increased: $H_0^{local} \equiv \frac{\dot{a}}{a}(today)$
  - apparent expansion rate appears to accelerate at late times: (extra curvature $\bar{q}_0$ of Hubble diagram) $\bar{q}_0^{local} \equiv \frac{\ddot{a}\,a}{\dot{a}^2}(today)$
- **Camarena & Marra 2020a,b jointly derived H_0 and $\bar{q}_0$ from SNe at redshifts 0.023 – 0.15**
  - $\bar{q}_0$ is 2x standard value of 0.55
    → suggestive of a local void
  - high local $\bar{q}_0$ missed in Kenworthy+ 2019 ($\bar{q}_0$ fixed at 0.55)
  - hint of dipole in Hubble diagram (Colin+ 2019, Migkas+ 2020, 2021)

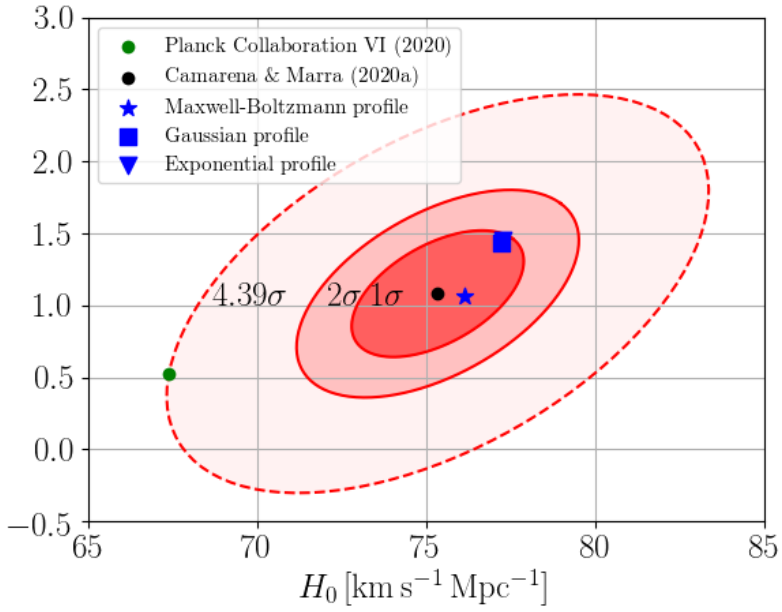

$H_0^{obs,local} = 75.35 \pm 1.68 \quad km/s/Mpc$

$\bar{q}_0^{obs,local} = 1.08 \pm 0.29$

$H_0^{model} = 76.15 \quad km/s/Mpc$

$\bar{q}_0^{model} = 1.07$

High local H_0 and $\bar{q}_0$ are explained naturally in MOND by outflow from a supervoid

Haslbauer, Banik & Kroupa 2020 (MNRAS, 499, 2845)

Comparison of data with ΛCDM & vHDM models

ΛCDM model

Observational constraints	Level of tension
KBC void (40 – 300 Mpc, 90% of sky)	6.04σ
H_0 (Riess+ 2019 & Wong+ 2020)	5.3σ

Parameters fixed by CMB

Combined tension: 7.09σ

Recent worsening of H_0 tension:
Early: Aiola+ 2020 (ACT)
Late: Pesce+ 2020 (Megamasers)

vHDM model

Observational constraints	Level of tension
KBC void (40 – 300 Mpc)	0.99σ
KBC void (600 – 800 Mpc)	0.97σ
H_0 and $\overline{q}_0$ from SNe data	0.20σ
H_0 from 7 strong lens time-delays	2.05σ
Motion of the LG wrt. CMB	2.34σ

3 free parameters
(initial void size & strength, g_{ext})
12 data points

Combined tension: 2.53σ

Conclusions

- Viable MOND cosmology (vHDM) can explain:
  - expansion history *a(t)* → BBN, CMB ($g \approx 20\ a_0$), non-standard structure growth at $z < 50$
  - Bullet Cluster and 30 virialized clusters (Angus+ 2010, MNRAS, 402, 395)
  - galaxy rotation curves unaffected by neutrinos if $m_\nu < 100\ eV/c^2$ (Angus+ 2010)

Conclusions

- Viable MOND cosmology (vHDM) can explain:
  - expansion history *a(t)* → BBN, CMB ($g \approx 20\ a_0$), non-standard structure growth at $z < 50$
  - Bullet Cluster and 30 virialized clusters (Angus+ 2010, MNRAS, 402, 395)
  - galaxy rotation curves unaffected by neutrinos if $m_\nu < 100$ eV/c^2 (Angus+ 2010)
- vHDM explains failures of ΛCDM on galaxy scales:
  - planes of satellites with high internal σ around MW (Pawlowski & Kroupa 2020), M31 (Ibata+ 2013, Sohn+ 2020, Pawlowski & Sohn 2021), Centaurus A (Müller+ 2018, 2021)
  - ΛCDM explanations rejected (Pawlowski+ 2014, MNRAS, 442, 2362)
  - other small scale failures (e.g. Peebles & Nusser 2010, Kroupa 2015, Peebles 2020, Banik+ 2021, Roshan+ 2021a,b, Haslbauer+ 2022)
- Large scale structure: KBC void and El Gordo cluster falsify ΛCDM but natural in vHDM
- Latest results: **tritonstation.com** and **darkmattercrisis.wordpress.com**

MOND review: Banik & Zhao 2022

Astrophysics > Cosmology and Nongalactic Astrophysics

[Submitted on 13 Oct 2021 (v1), last revised 24 Nov 2021 (this version, v3)]

From galactic bars to the Hubble tension – weighing up the astrophysical evidence for Milgromian gravity

Indranil Banik, Hongsheng Zhao

Astronomical observations reveal a major deficiency in our understanding of physics – the detectable mass is insufficient to explain the observed motions in a huge variety of systems given our current understanding of gravity, Einstein's General theory of Relativity (GR). This missing gravity problem may indicate a breakdown of GR at low accelerations, as postulated by Milgromian dynamics (MOND). We review the MOND theory and its consequences, including in a cosmological context where we advocate a hybrid approach involving light sterile neutrinos to address MOND's cluster-scale issues. We then test the novel predictions of MOND using evidence from galaxies, galaxy groups, galaxy clusters, and the large scale structure of the Universe. We also consider whether the standard cosmological paradigm (ΛCDM) can explain the observations, and review several previously published highly significant falsifications of it. Our overall assessment considers both the extent to which the data agree with each theory and how much flexibility each has when accommodating the data, with the gold standard being a clear a priori prediction not informed by the data in question. We also consider some future tests, including on scales much smaller than galaxies. Our conclusion is that MOND is favoured by a wealth of data across a huge range of astrophysical scales, ranging from the kpc scales of galactic bars to the Gpc scale of the local supervoid and the Hubble tension, which is alleviated in MOND through enhanced cosmic variance.

Comments: Invited review for special issue of Symmetry on modified gravity. 80 pages, 34 figures, 6 tables. Revised in response to comments. Not yet submitted, comments welcome until end of November 2021

Subjects: **Cosmology and Nongalactic Astrophysics (astro-ph.CO)**; Astrophysics of Galaxies (astro-ph.GA)

Cite as: arXiv:2110.06936 **[astro-ph.CO]**

(or arXiv:2110.06936v3 **[astro-ph.CO]** for this version)

Submission history

From: Indranil Banik [view email]

[v1] Wed, 13 Oct 2021 18:00:01 UTC (5,624 KB)

[v2] Thu, 28 Oct 2021 17:38:51 UTC (5,633 KB)

[v3] Wed, 24 Nov 2021 05:51:30 UTC (5,658 KB)

Appendix

Outlook

- **Enable standard RAMSES hydrodynamics and cosmology to study galaxy formation with Phantom of RAMSES (PoR MOND patch, Lüghausen+ 2015, user guide: Nagesh+ 2021, CaJPh, 99, 607)**
  - Simulation by Nils Wittenburg
  - SPODYR group (University of Bonn)
- **Self-consistent cosmological MOND simulation on much larger scales**
  - study formation of voids in a large simulation box
  - What does a typical KBC-like void look like?
  - cosmic variance

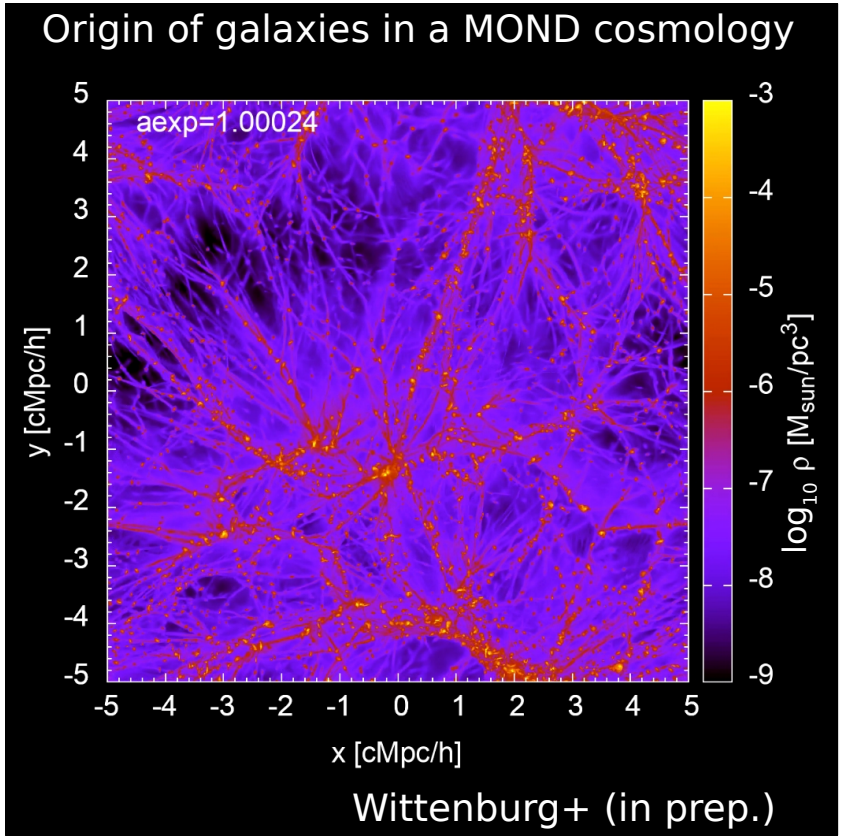

The fake inclination effect in MOND

- **AGC 114905 claimed to have rotation curve well below MOND expectations**
- $$v_c \propto \frac{1}{\sin i}$$

  ***i* estimated at 32° from isophote shapes**
- **But isophotes can appear elliptical even if galaxy face-on, because even LSB discs are self-gravitating and can sustain non-axisymmetry**
- **Rotation curve much higher and consistent with MOND if galaxy almost face-on (i = 11°)**
- **Significant non-axisymmetry would be unusual in ΛCDM if the dark halo dominates (Sellwood & Sanders 2022, ArXiv: 2202.08678)**

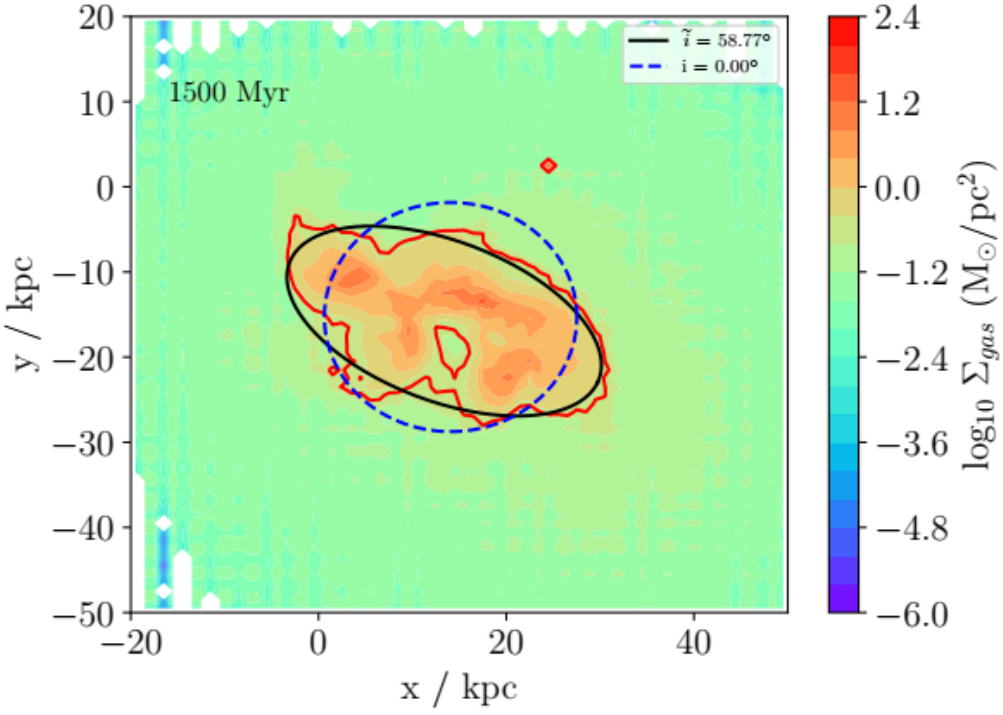

Credit: I. Banik et al., resubmitted

Haslbauer+ 2022 (ApJ, 925, 183)

- **High fraction of thin disk galaxies in observed Universe contradicts expectations from TNG50**
- **Improving resolution will not solve the problem**

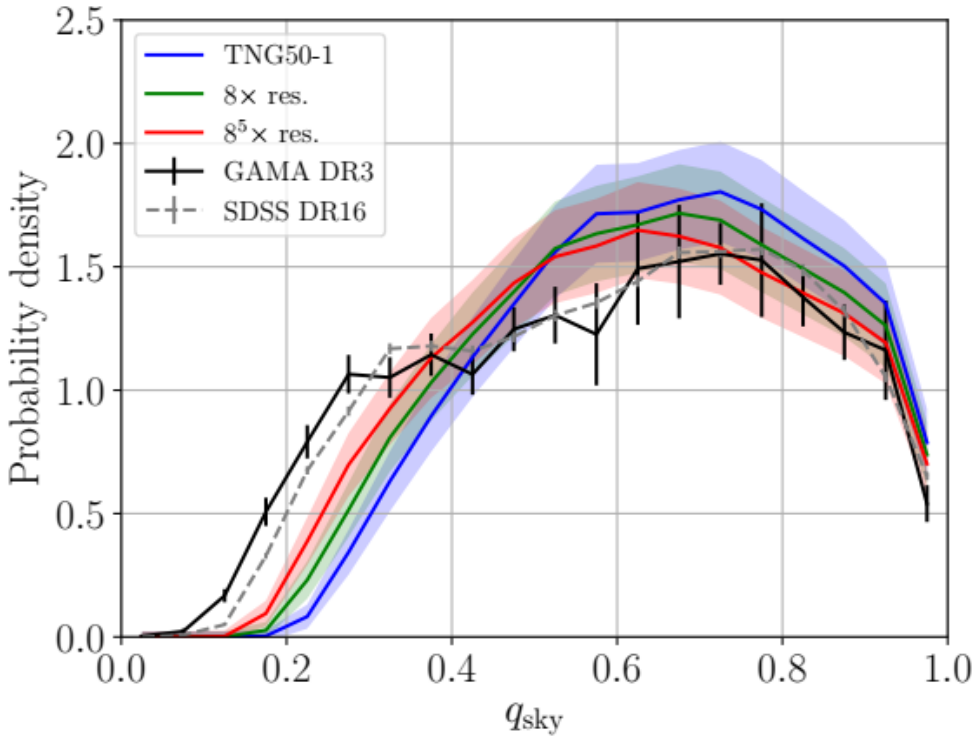

KBC 2013, ApJ, 775, 62: luminosity function

- **Shape of luminosity function clearly determined based on 57-75% of luminosity function**
- **Normalization systematically lower at low z**
- **Density contrast similar between magnitude bins**

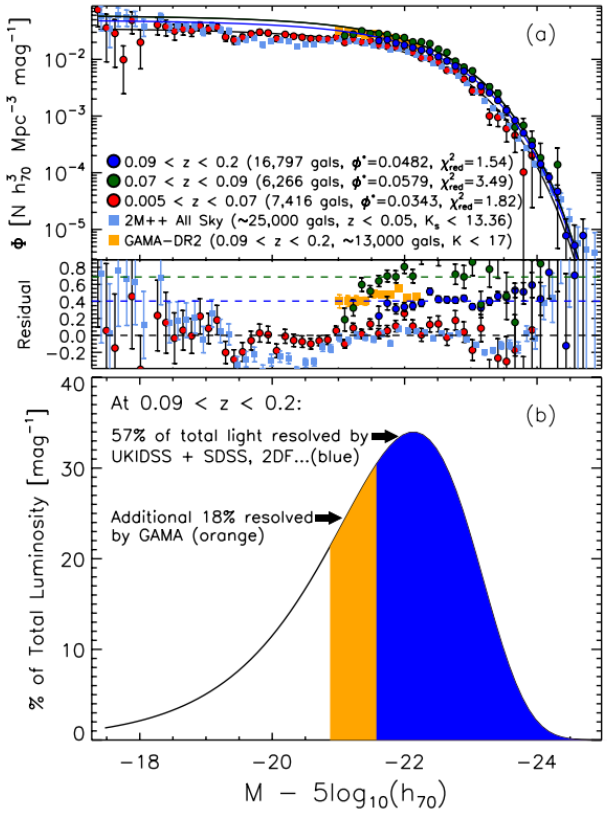

The KBC void in ΛCDM

- **Millennium (MXXL) simulation (Angulo+ 2012)**
  - ΛCDM simulation consistent with WMAP-1 parameters
  - biggest suitable simulation (box size of 4.1 Gpc)
  - Stellar masses assigned semi-analytically

- **Mimic observations (2M++ survey)**
  - select subhaloes with $M_* > 1e10\ M_\odot/h$ at $z = 0$
  - calculate luminosity density contrasts over (40 – 300) Mpc for 1e6 vantage points

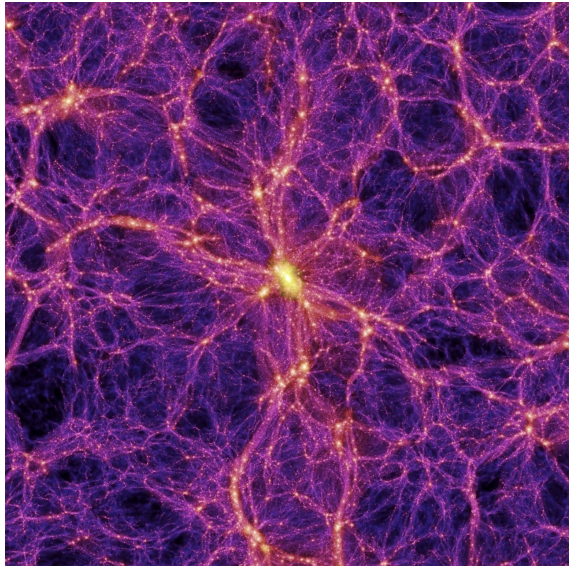

Source: Millennium simulation

⇒ Expected rms density fluctuations for scale-invariant spectrum: 0.032

Observed density fluctuation: 0.46±0.06

Peculiar velocity field

- **Only half of the void rms size is shown**
- **The entire void is moving due to gravity from beyond the void**
- **Partial cancellation between void motion and internal velocities**
- **Large region with peculiar velocity $v_{tot} < v_{LG} = 627$ km/s ($\approx 0.015\ a_0/H_0$)**
  - Local Group (LG) is off-centered
  - LG not at a special position
- **High peculiar velocities towards void edge consistent with kinematic Sunyaev-Zel'dovich effect (Hoscheit & Barger 2018, Ding et al. 2020)**

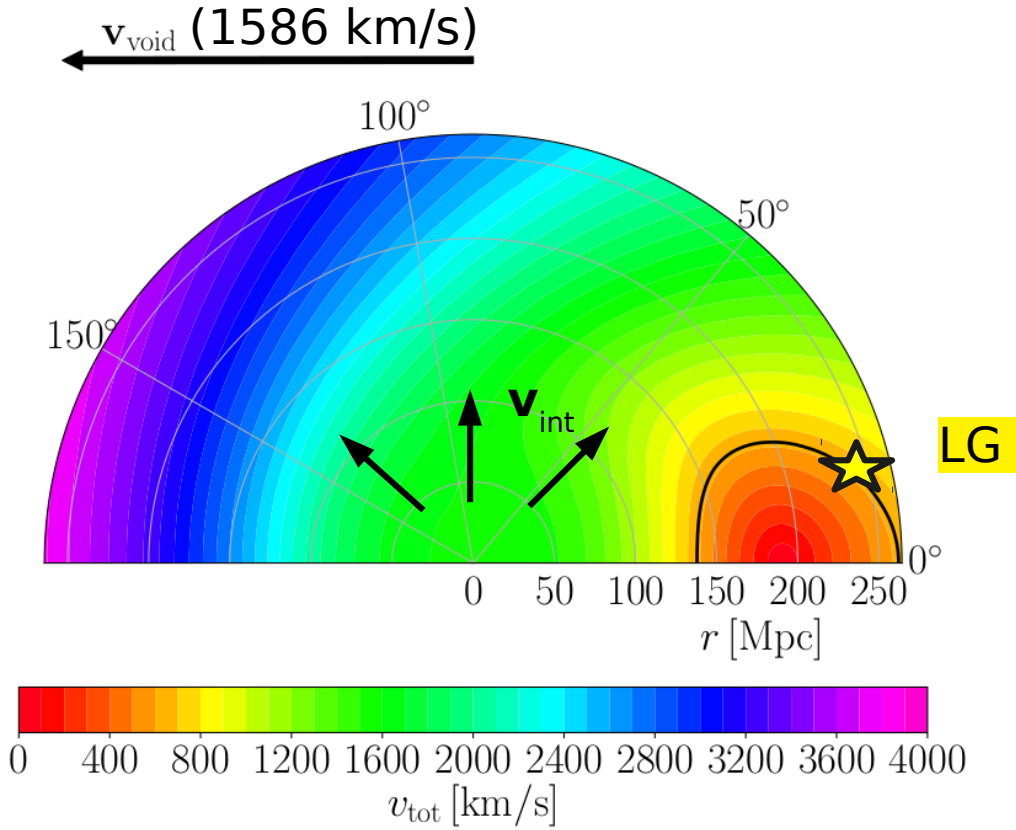

Outlook: Stellar wide binary (WB) test

- **WBs with separation r > 3 kAU (like Proxima Centauri, Sun's nearest star)**
- **Orbital accelerations < a_0 (MOND regime)**
  - MOND boosts orbital velocities by **20%** in Solar neighbourhood
- **Accurate observations of about 500 WBs necessary (Banik & Zhao 2018)**
  - e.g. Gaia data release 3, Theia mission
- **Statistical treatment of undetected close companions to WBs necessary**
  - WBs with r < 3 kAU should be similar to WBs with r > 3 kAU in Newton
  - Low r systems and high-velocity tail constrain close binary population
  - For a detailed plan, see ArXiv: 2109.03827
- **MOND without EFE is ruled out by the WB test (Pittordis & Sutherland 2019)**

Terrestrial evidence for light sterile neutrinos

- **Sterile neutrinos proposed to explain ordinary neutrino oscillations & their non-zero rest mass (seesaw mechanism)**
- **Hints of sterile neutrino found by MiniBooNE**

  (Aguilar-Arevalo+ 2018, Phys. Rev. Lett. 121, 221801)
- **Must avoid prior limit that $m_\nu < 10$ eV/c² as terrestrial experiments are so far quite compatible with slightly larger mass**
- **Sterile neutrinos allowed by MicroBooNE (ArXiv: 2111.10359)**

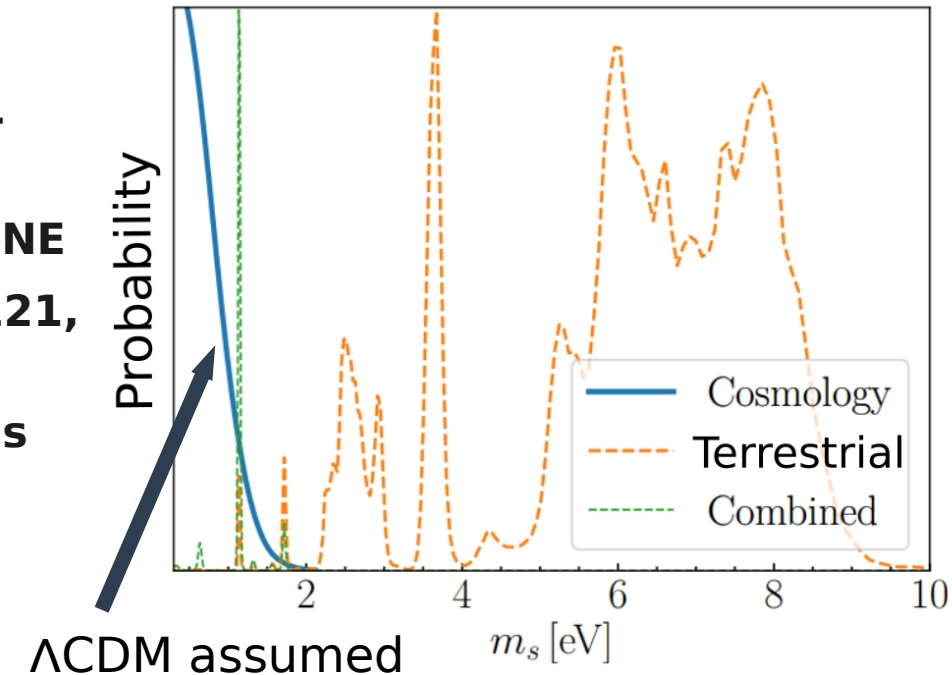

Archidiacono+ 2020 (JCAP, 12, 029)

Fraction of disk galaxies with a bar

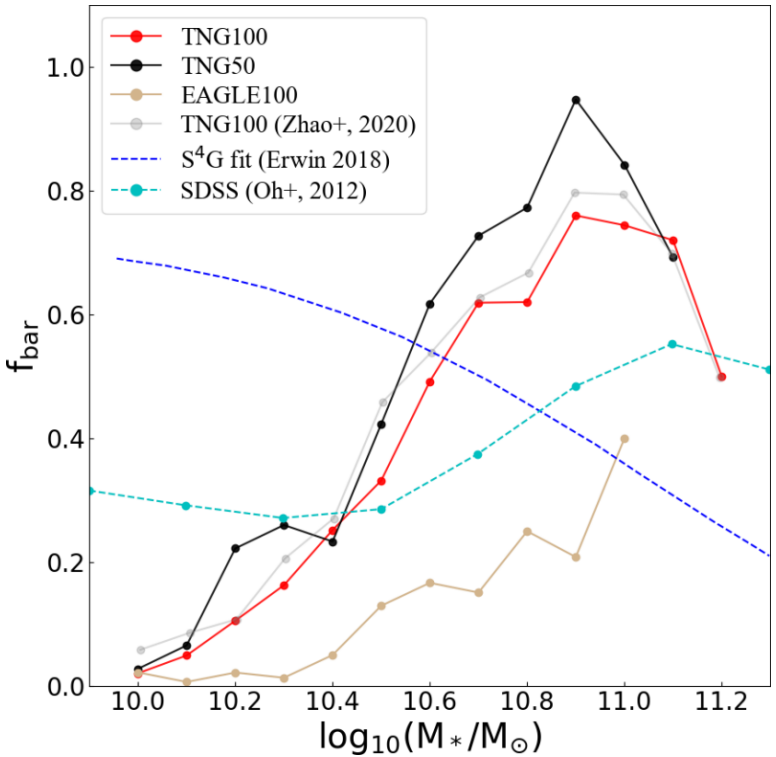

S4G data has much higher resolution (based on Spitzer)

Results converged (similar between TNG50 and TNG100)

Similar results found in NewHorizon simulation by Reddish+ 2022 (MNRAS, in press, stac494)

Colgáin (2019)

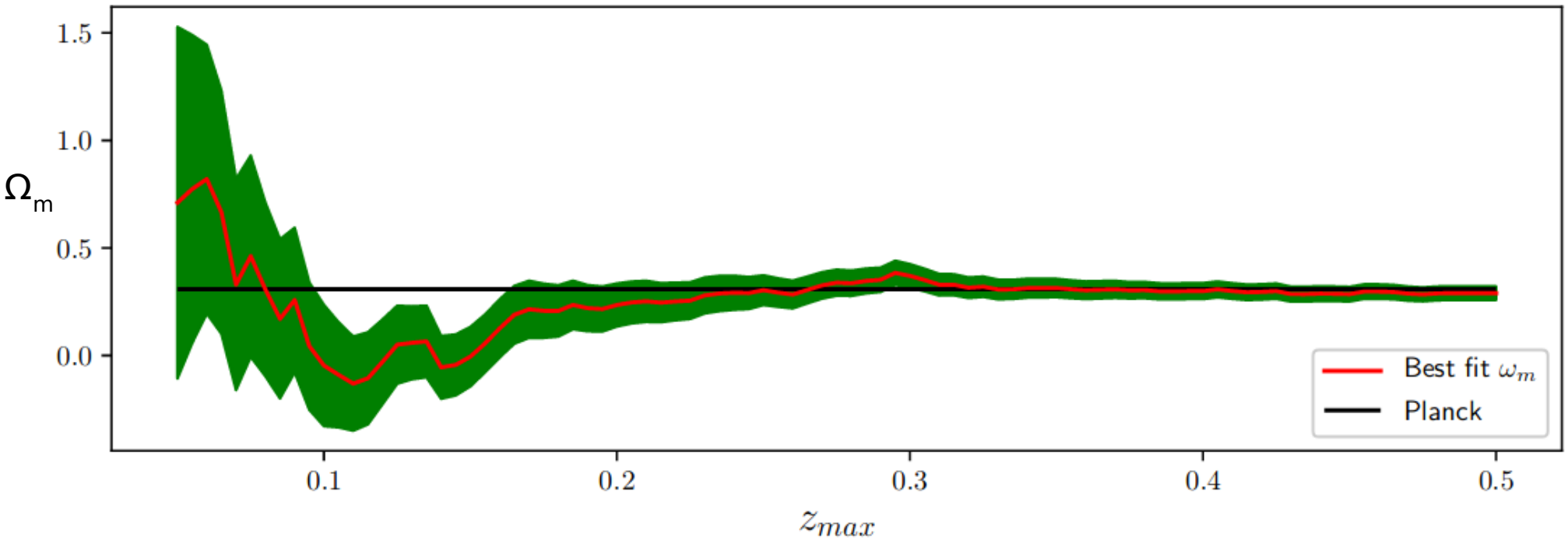

Results: Gaussianity test of the selected density fluctuations in the MXXL simulation

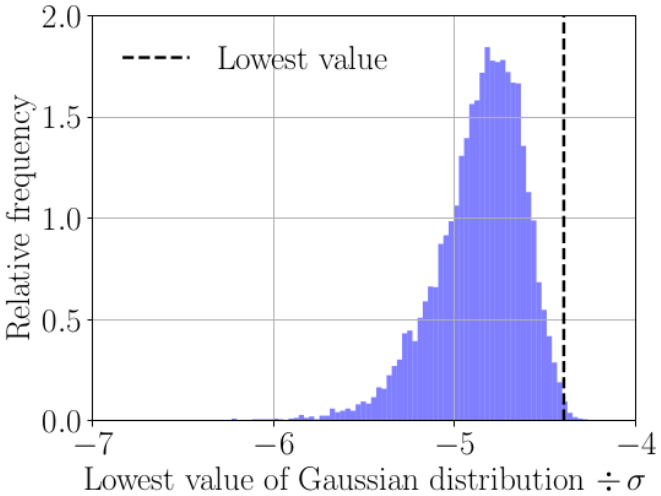

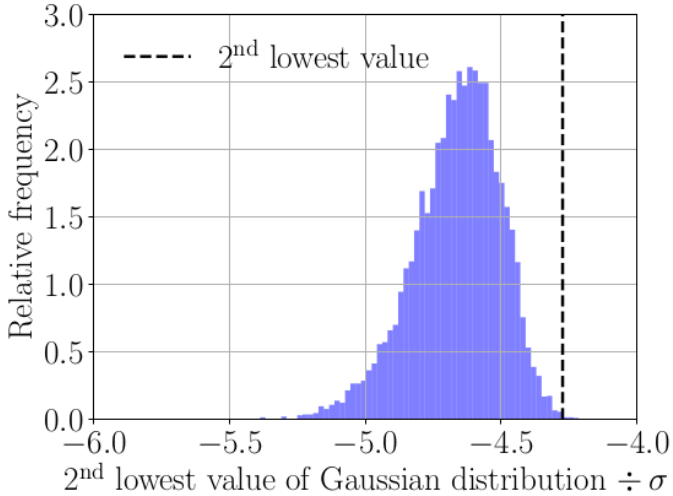

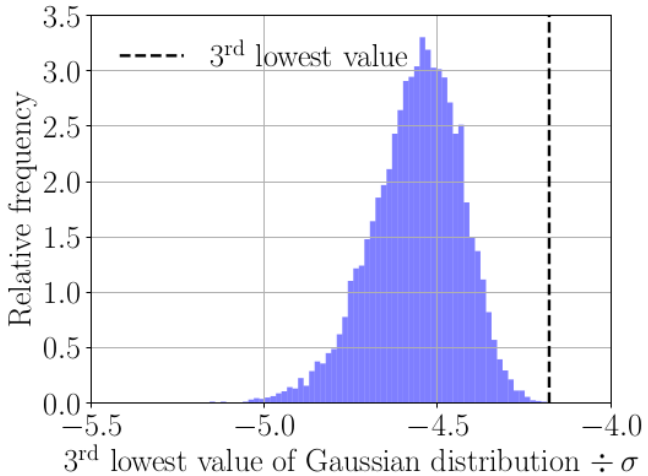

Results: H_0 from strong lensed systems

- **Empirically, light deflection in strong lenses works similar to General Relativity for the same non-relativistic** g **(Collett+ 2018)**
- **Relativistic MOND theories exist where gravitational waves travel at the speed of light (Skordis & Złośnik 2019)**
- **Decreasing inferred H_0 with lens redshift (Wong+2020) evident at 1.9σ**

  ⇒ curvature in Hubble diagram (like with SNe)
- **Consistent with MOND model (2.05σ), but suggestive of a larger void than KBC data**

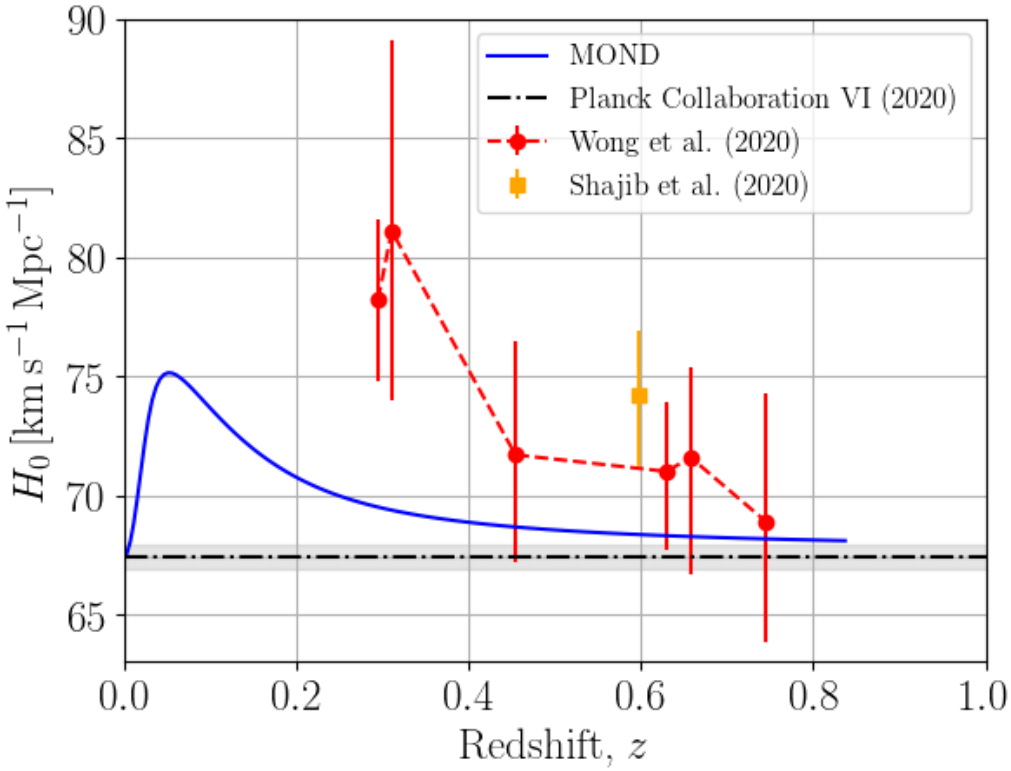

vHDM framework: apparent expansion history

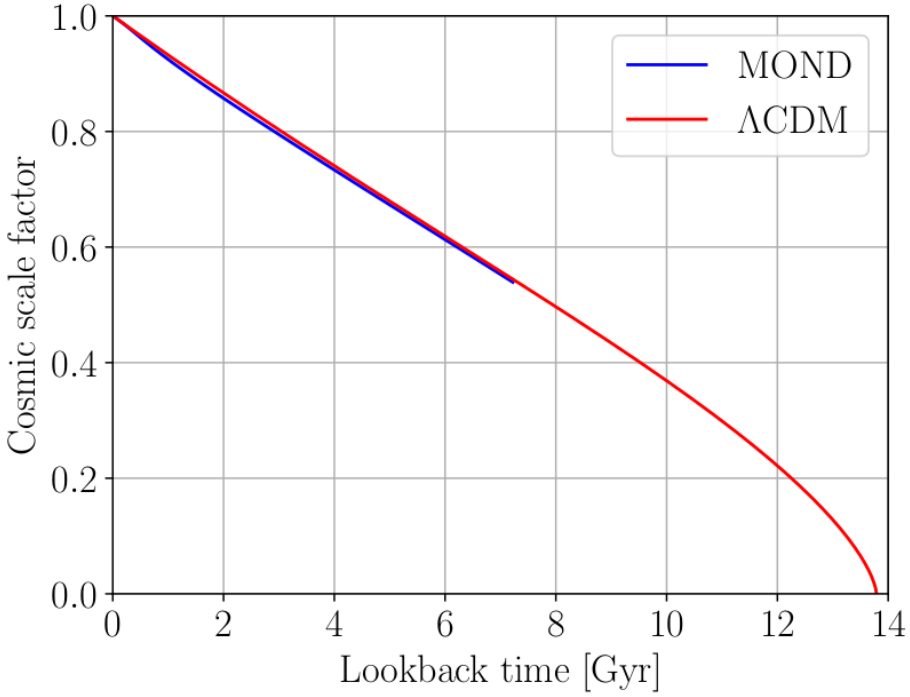

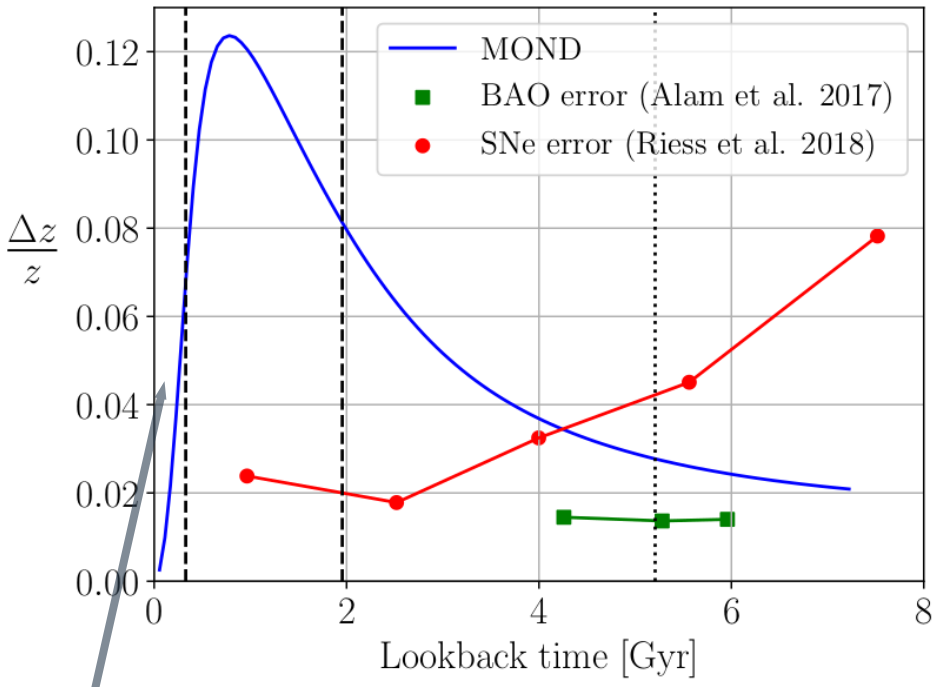

Hubble flow velocity very small: $v_{Hubble} \not\gg v_{pec}$
(e.g. Kim+2020)

Results:

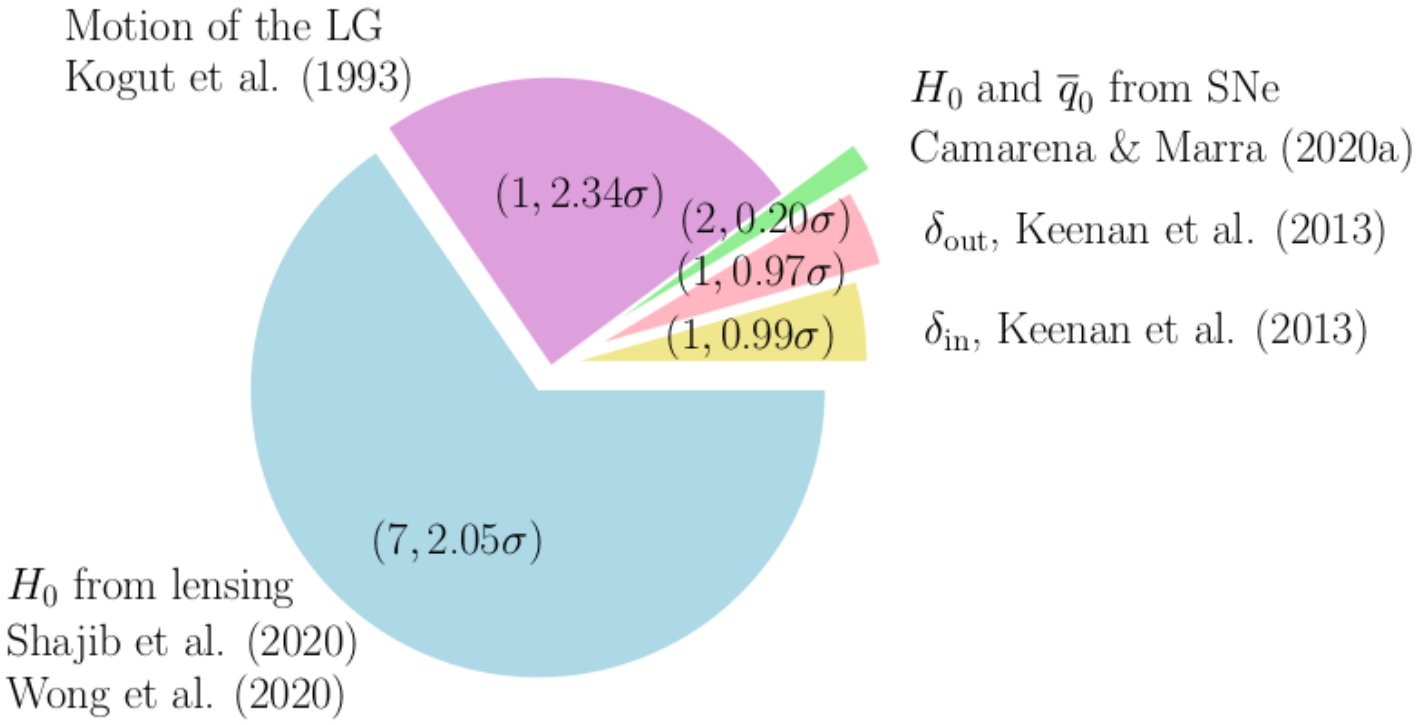
Motion of the LG
Kogut et al. (1993)
H_0 and $\overline{q}_0$ from SNe
Camarena & Marra (2020a)
$\delta_{\rm out}$, Keenan et al. (2013)
$\delta_{\rm in}$, Keenan et al. (2013)
H_0 from lensing
Shajib et al. (2020)
Wong et al. (2020)
$(1, 2.34\sigma)$
$(2, 0.20\sigma)$
$(1, 0.97\sigma)$
$(1, 0.99\sigma)$
$(7, 2.05\sigma)$

Results:

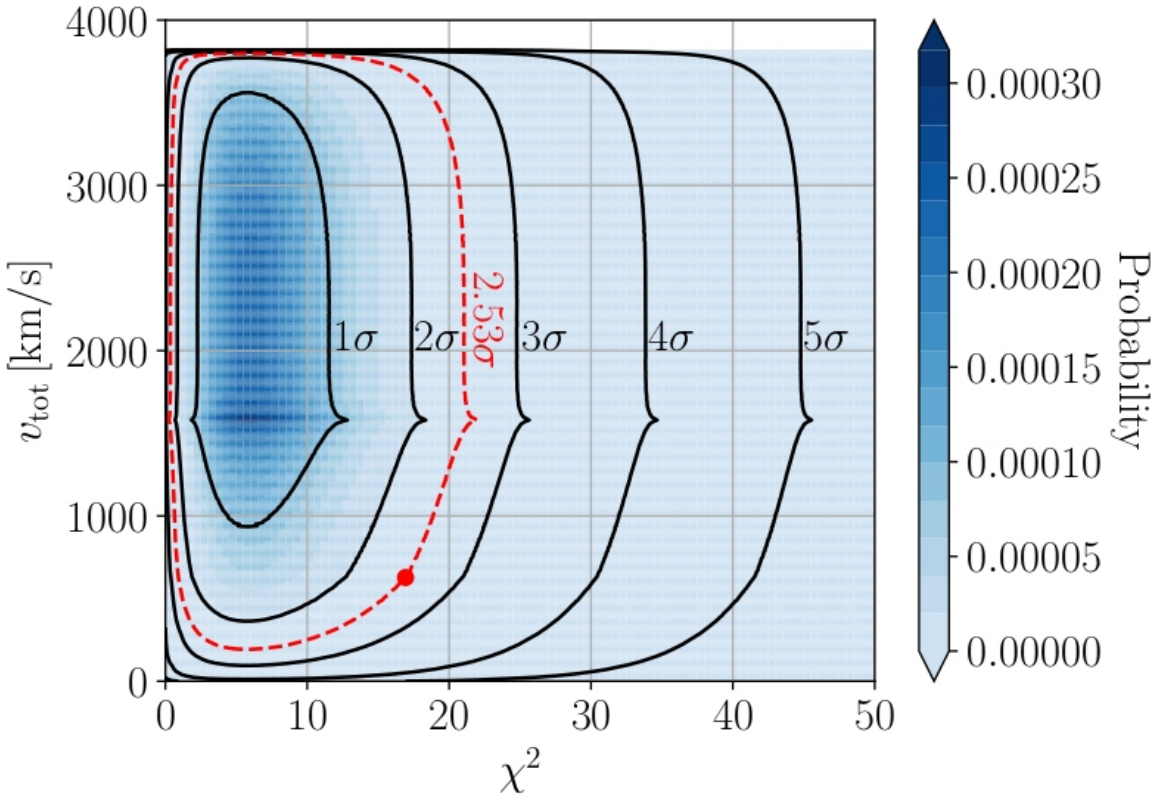
4000
3000
2000
1000
0
$v_{\rm tot}$ [km/s]
0
10
20
30
40
50
χ^2
1σ
2σ
2.53σ
3σ
4σ
5σ
0.00030
0.00025
0.00020
0.00015
0.00010
0.00005
0.00000
Probability

Results:

Maxwell-Boltzmann density profile, $g_{ext} = 0.055\,a_0$, $r_{void} = 228.2\,\mathrm{cMpc}$, $\alpha_{void} = 3.76 \times 10^{-5}$, $v_{void} = 1586\,\mathrm{km\,s^{-1}}$, $r_{void}^{rms} = 528.7\,\mathrm{Mpc}$, $n_{EFE} = 0$						
Parameter	H_0^{local} [km s^{-1} Mpc^{-1}]	q_0^{local}	$H_0^{lensing}$ [km s^{-1} Mpc^{-1}]	v_{LG} [km s^{-1}]	δ_{in}	δ_{out}
Observations	75.35 ± 1.68	1.08 ± 0.29	––	627	0.254 ± 0.083	-0.052 ± 0.105
MOND model	76.15	1.07	See Figure 7	See Figure 8	0.172	0.050
χ^2	0.34		14.66	––	0.99	0.94
Degrees of freedom	2		7	––	1	1
χ (1D Gaussian equivalent)	0.20		2.05	2.34	0.99	0.97
Gaussian density profile, $g_{ext} = 0.070\,a_0$, $r_{void} = 1030.0\,\mathrm{cMpc}$, $\alpha_{void} = 3.76 \times 10^{-5}$, $v_{void} = 2018\,\mathrm{km\,s^{-1}}$, $r_{void}^{rms} = 744.7\,\mathrm{Mpc}$, $n_{EFE} = 0$						
Parameter	H_0^{local} [km s^{-1} Mpc^{-1}]	q_0^{local}	$H_0^{lensing}$ [km s^{-1} Mpc^{-1}]	v_{LG} [km s^{-1}]	δ_{in}	δ_{out}
Observations	75.35 ± 1.68	1.08 ± 0.29	––	627	0.274 ± 0.081	-0.085 ± 0.108
MOND model	77.24	1.43	––	––	0.155	0.078
χ^2	1.79		12.74	––	2.19	2.26
Degrees of freedom	2		7	––	1	1
χ (1D Gaussian equivalent)	0.83		1.76	2.35	1.48	1.50
Exponential density profile, $g_{ext} = 0.080\,a_0$, $r_{void} = 1030.0\,\mathrm{cMpc}$, $\alpha_{void} = 7.56 \times 10^{-5}$, $v_{void} = 2307\,\mathrm{km\,s^{-1}}$, $r_{void}^{rms} = 730.4\,\mathrm{Mpc}$, $n_{EFE} = 0$						
Parameter	H_0^{local} [km s^{-1} Mpc^{-1}]	q_0^{local}	$H_0^{lensing}$ [km s^{-1} Mpc^{-1}]	v_{LG} [km s^{-1}]	δ_{in}	δ_{out}
Observations	75.35 ± 1.68	1.08 ± 0.29	––	627	0.276 ± 0.080	-0.078 ± 0.108
MOND model	77.25	1.46	––	––	0.158	0.073
χ^2	1.98		13.19	––	2.17	1.97
Degrees of freedom	2		7	––	1	1
χ (1D Gaussian equivalent)	0.89		1.83	2.47	1.47	1.40

Results:

Maxwell-Boltzmann profile

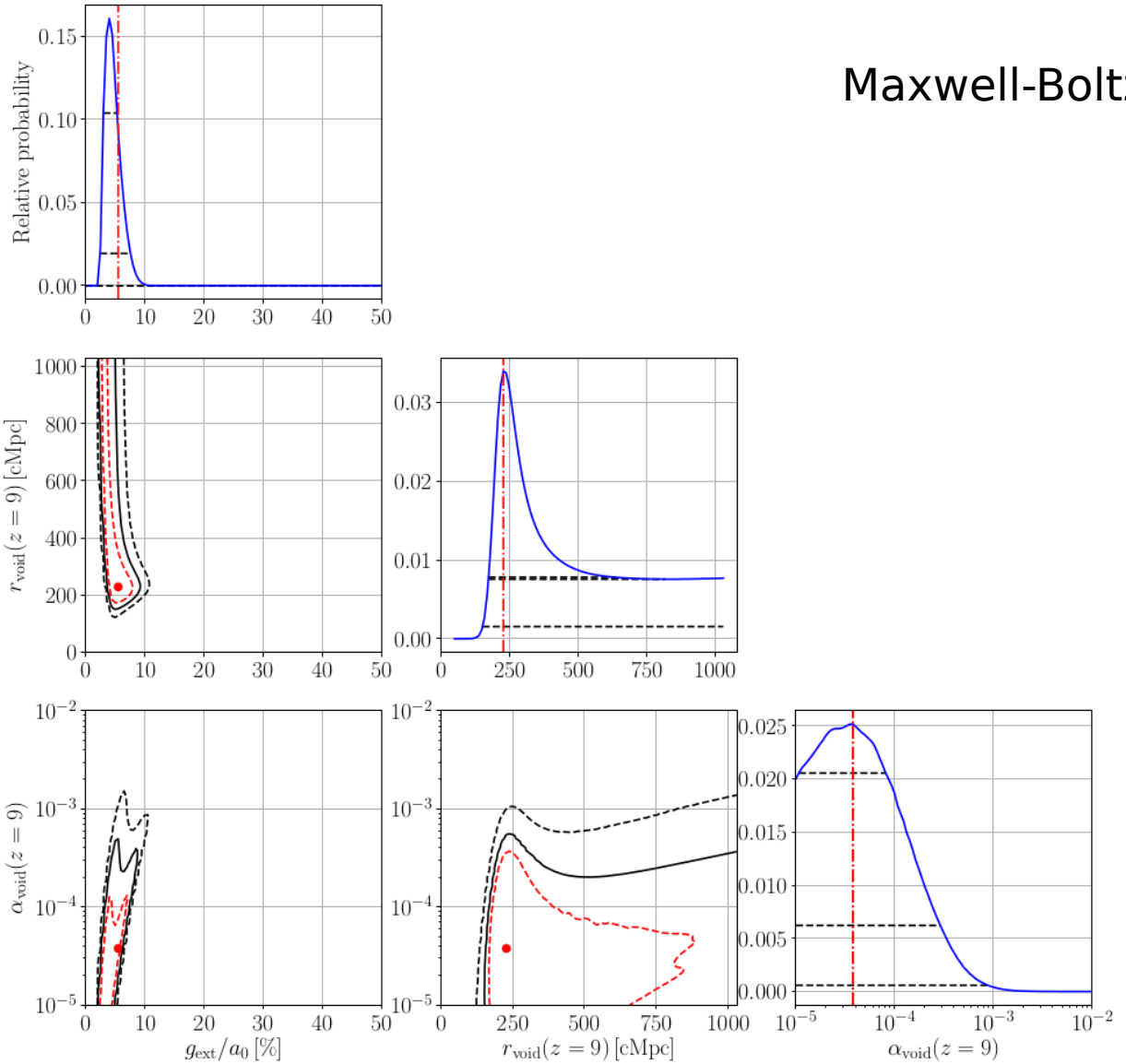

Results:

Gaussian profile

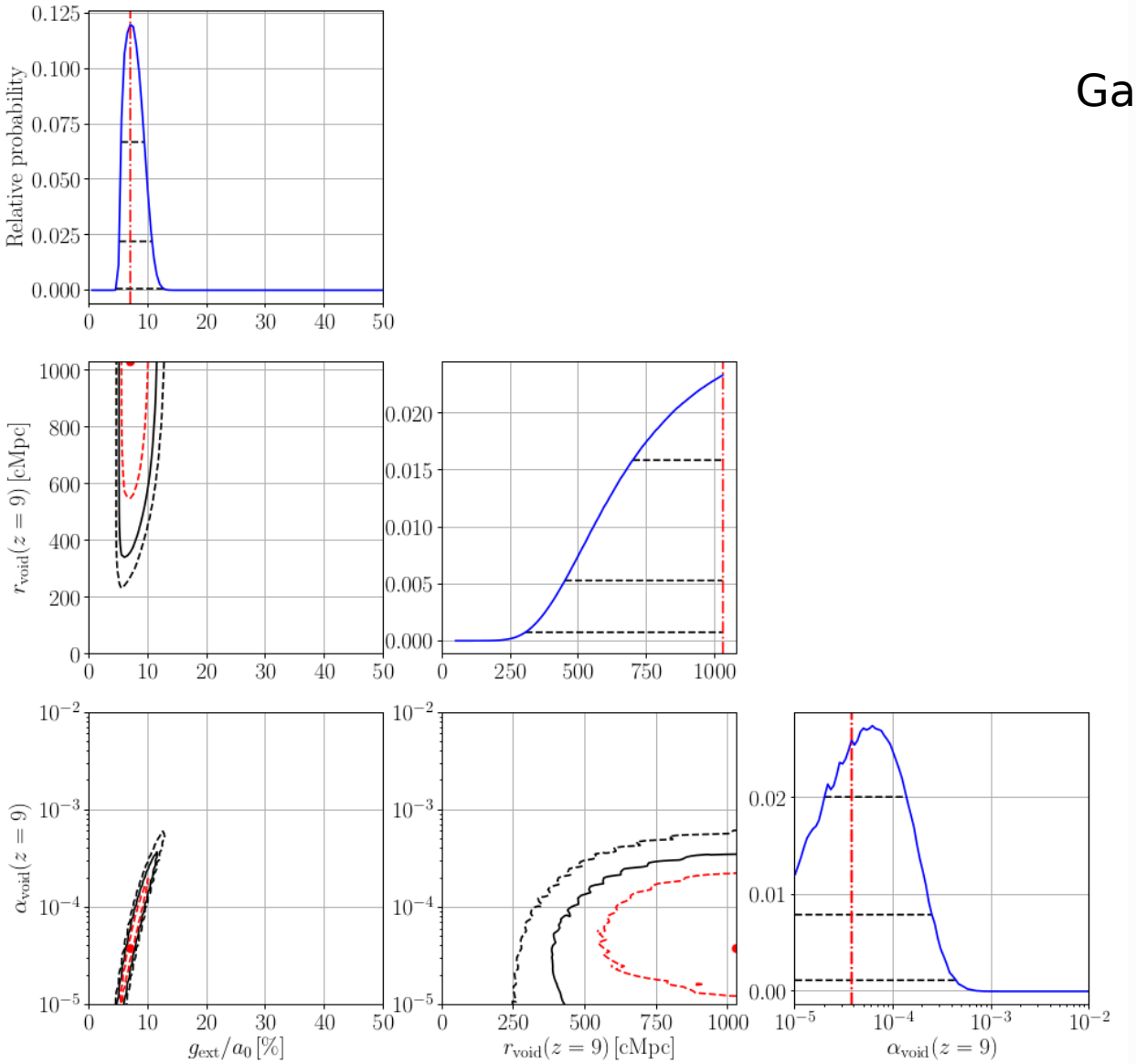

Results: Hubble field effect

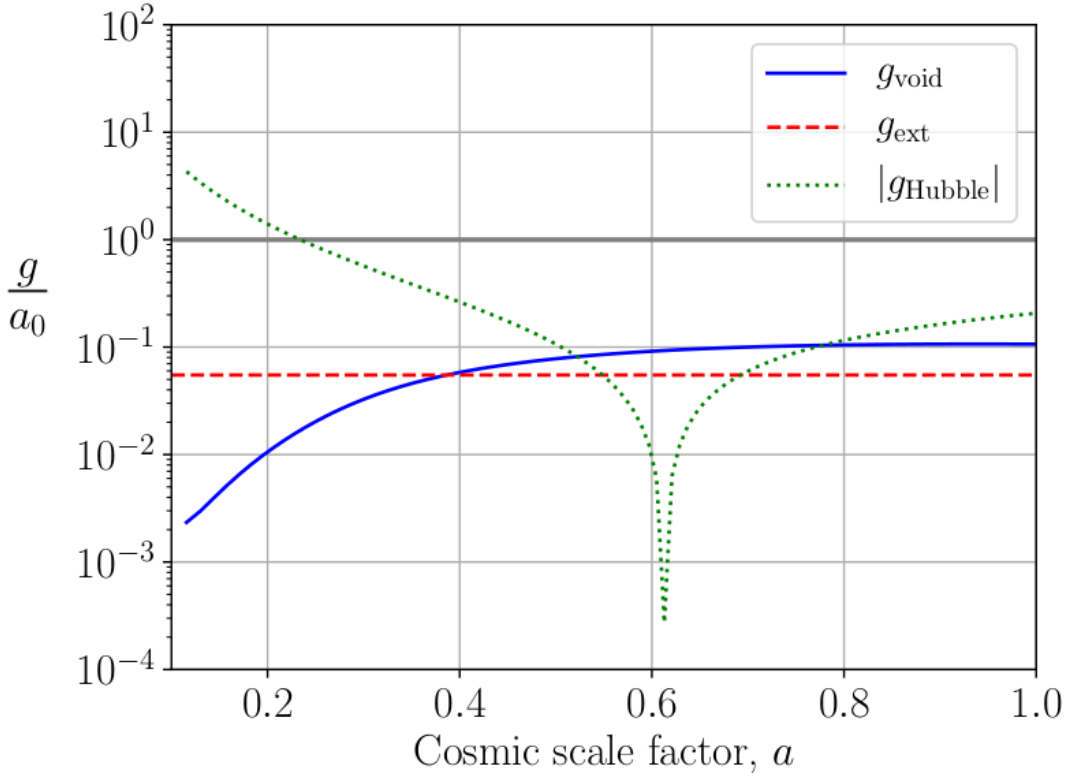

Results: Time-dependent external field effect

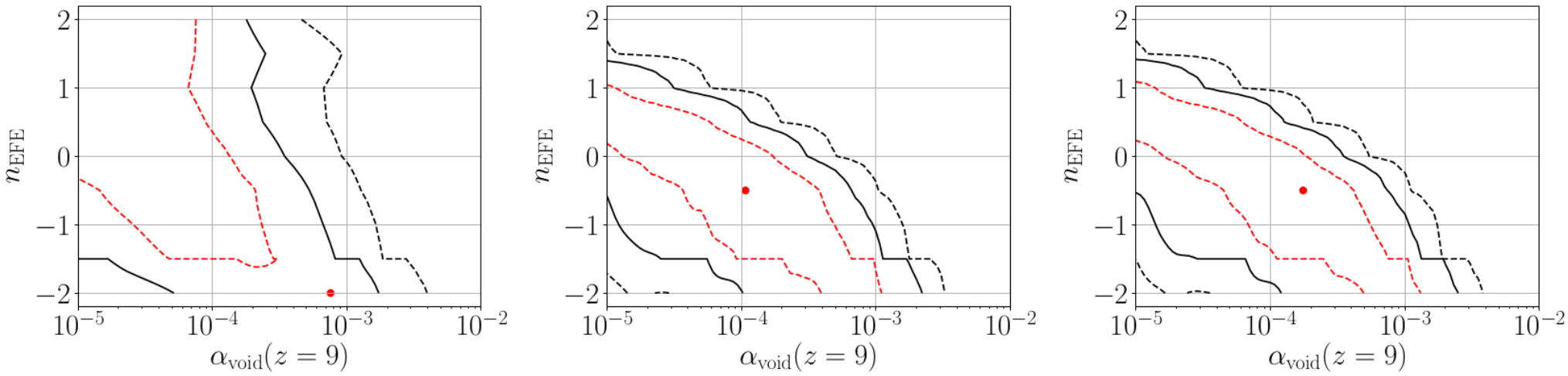

Figure 14. Marginalized posterior distribution of the indicated model parameters based on 9×10^6 MOND models for a Maxwell-Boltzmann (left), Gaussian (middle), and exponential (right) initial profile. The red dashed, black solid, and black dashed lines mark the 1σ, 2σ, and 3σ confidence levels, respectively. A stronger EFE in the past ($n_{\rm EFE} < 0$) requires a stronger initial void strength at $z = 9$. The red dots mark the best-fitting models: $g_{\rm ext} = 0.030\,a_0$, $r_{\rm void} = 218.3\,{\rm cMpc}$, $\alpha_{\rm void} = 7.56 \times 10^{-4}$, $n_{\rm EFE} = -2$ (Maxwell-Boltzmann profile, left-hand panel); $g_{\rm ext} = 0.065\,a_0$, $r_{\rm void} = 1030.0\,{\rm cMpc}$, $\alpha_{\rm void} = 1.07 \times 10^{-4}$, $n_{\rm EFE} = -0.5$ (Gaussian profile, middle panel); and $g_{\rm ext} = 0.070\,a_0$, $r_{\rm void} = 1030.0\,{\rm cMpc}$, $\alpha_{\rm void} = 1.75 \times 10^{-4}$, $n_{\rm EFE} = -0.5$ (exponential profile, right-hand panel).

Results: Time-dependent external field effect